# Signaling Behaviors of Intrinsically Disordered Proteins

Lara Clemens

Make a title page and better title

# Contents


**1 Abstract** **5**

**2 Introduction/Background/Motivation** **5**

2.1 Intrinsically Disordered Proteins . . . . . 5

2.2 T Cell Receptor Zeta Chain . . . . . 5

2.3 Multisite Phosphorylation . . . . . 6

2.4 Previous Modeling Attempts - FJC as Model for IDPs . . . . . 6

2.5 The Big Question . . . . . 7

**3 Model Development** **7**

3.1 Freely Jointed Chain . . . . . 7

3.2 Theoretical results . . . . . 8

3.3 Code Validation . . . . . 9

3.3.1 Root-mean-square end-to-end distance . . . . . 9

3.3.2 $R_{ee}$ Distribution . . . . . 9

3.3.3 Occlusion Probability of End Site VS Analytical Result . . . . . 10

3.4 Case Study: T Cell Receptor Zeta Chain . . . . . 10

**4 Local structuring of disordered signaling proteins gives rise to cooperativity and sequential binding** **11**

4.1 Introduction . . . . . 11

4.2 Model and Methods . . . . . 12

4.3 Results . . . . . 12

4.3.1 Surface presence influences polymer configuration . . . . . 12

4.3.2 Disorder inhibits ligand binding . . . . . 13

4.3.3 Cooperativity may arise from local structuring in intrinsically disordered proteins . . . 14

4.3.4 Sequential binding naturally arises from polymer characteristics . . . . . 15

4.3.5 Negative cooperativity may arise from local disordering of proteins . . . . . 17

4.3.6 Future Work: Quantifying cooperativity from reversible phoshphorylation with Hill coefficients . . . . . 17

4.3.7 Future Work: Exploring sequence of binding from dephosphorylation and reversible phosphorylation . . . . . 18

4.4 Discussion . . . 18

**5 Electrostatics** **18**

5.1 Introduction . . . 18

5.2 Model and Methods . . . 18

5.2.1 Electrostatic Potentials . . . 20

5.3 Results . . . 21

5.3.1 Model in which basic residues and tyrosines have similar energetics reveals puzzle in existing data . . . 21

5.3.2 Initial parameter exploration of more general energetic model yields fit to polymer distribution . . . 21

5.3.3 Future Work . . . 23

5.4 Discussion? . . . 24

**6 Results: Simultaneous Binding** **24**

6.1 Introduction . . . 24

6.2 Model and Methods . . . 24

6.3 Results . . . 24

6.3.1 Negative cooperativity arises from simultaneous binding of ligands to an IDP . . . 24

6.3.2 Future Work: Sequence of binding multiple ligands . . . 27

6.3.3 Future Work: Multiple chains towards a full model of a T cell receptor signalosome . . . 28

6.4 Discussion . . . 28

**7 Role of the surface on tether-tether reactions within a signaling cluster** **28**

7.1 Introduction . . . 28

7.1.1 Tethering . . . 28

7.1.2 SHP-1 . . . 28

7.2 Model and Methods . . . 29

7.2.1 Model Tethers as Freely Jointed Chain . . . 29

7.2.2 SHP1 Parameters . . . 29

7.2.3 Curve Fitting . . . 33

7.3 Results . . . 34

7.3.1 Accessibility of a reaction site is reduced by the presence of a surface . . . 34

7.3.2 Reactions between tethered reactants are net enhanced by a surface . . . . . 34
7.3.3 Reach parameter is unaffected by presence of surface . . . . . 36
7.3.4 Matrix-bound versus surface-bound experiments confirm model predictions . . . . . 38
7.3.5 Future Work: Catalysis surface factor $\kappa_{cat}^{(teth2teth)}$ versus $l_C$ and/or versus $r_{ligand}$ . . . 38
7.4 Discussion? . . . . . 39

**8 Timeline** **39**

**9 Appendix** **39**

9.1 Model Modifications . . . . . 39
9.1.1 Stiffening . . . . . 39
9.1.2 Electrostatics . . . . . 39
9.1.3 LJ Parameter Optimization . . . . . 40
9.1.4 Simultaneous Binding . . . . . 41
9.2 Assumptions . . . . . 42
9.3 Gillespie Algorithm . . . . . 42

# 1 Abstract

Disordered proteins are present in at least 40% of human proteins, including signaling molecules. What functionality disordered proteins contribute to a signaling network and how is not well understood. I don't like this sentence Here we explore how disordered proteins impact singular and multi-site ligand binding through a variety of disorder-specific phenomenons. In addition to basic properties of disordered protein interactions, we investigate disorder-to-order transitions, electrostatic membrane association, simultaneous ligand binding and effects of surface presence. We find that disordered proteins may create positive or negative cooperativity and intrinsic sequential binding. These effects are influenced by the length of the disordered protein, size of the binding ligand, location of the binding sites along the polymer and presence or absence of a surface. Intrinsically disordered proteins themselves may therefore act as signaling modules that contribute complex signaling behavior to a network.

# 2 Introduction/Background/Motivation

Traditionally, studies of protein function have gone hand-in-hand with studies of protein structure. Proteins such as hemoglobin exhibit complicated behavior, such as cooperativity, by modifying their structure. The cooperative transition of hemoglobin from a closed to open state is well studied with the aid of crystallography and other structure elucidation tools. CITE

Of more recent interest is the behavior of molecules that cannot be crystallized. These proteins lack a defined structure and instead are capable of assuming many different conformations. Although examples of intrinsically disordered proteins (IDPs) have been reported since the 1970s, it was only in the past two decades that they became a focus of major research. [**Dunker2008**]

As our understanding of disordered proteins develops, so too will our understanding of a variety of cellular behaviors. These studies will elucidate aspects of signaling, cytoskeleton formation, clustered reactions, and really. I need a fourth function.. Investigations into how disordered proteins mediate each of these processes may lead to new drug targets or introduce new directions for synthetic biology.

## 2.1 Intrinsically Disordered Proteins

Studies have shown that disordered proteins or disordered domains are present in at least 40% of human proteins, including those involved with signal propagation.[4] General functions of IDPs include as tethers between two globular domains cite, receptor subunits in signaling pathways cite, tethers to the membrane cite, and facilitators to actin polymerization cite - formin. Given the ubiquitous nature of IDPs, many questions arise: How does their existence influence cellular functions such as biochemical reactions, signaling networks, or cytoskeletal structure? Are there any benefits to being disordered over structured? and Can IDPs exhibit the same complicated behavior as structured proteins?

## 2.2 T Cell Receptor Zeta Chain

One example of an intrinsically disordered protein is the CD3 $\zeta$ chain, a subunit of a receptor in T cells. This molecule facilitates signal propagation in the T Cell Receptor (TCR) network in the immune system. An antigen binding to the extracellular regions of the TCR creates a signal transmitted via a chain of events into the cell to the intracellular components of the TCR including the CD3$\zeta$ chain. An individual CD3$\zeta$ chain undergoes multiple phosphorylation by kinase Lck before another molecule, ZAP-70 can attach and propagate the signal downstream. This pathway ultimately regulates T-cell cell fate decisions through cytokines production, (i.e. interleukin-2). Cite - Cell Signal.com??

TCR CD3$\zeta$ is one of six disordered chains composing the TCR intracellular region. Experiments with a single mouse CD3$\zeta$ have shown that the rate of the last phosphorylation event is about one hundred times faster than the rate of the first phosphorylation event. single, right? CITE Omer To achieve this kind of enhancement, we would expect cooperativity to occur between phosphorylation events.

Since IDPs lack a consistent, rigid structure, they must fluctuate between multiple conformations. If we assume IDPs have no structure at all, then the protein may be in any conformation at any time and in fact would sample all of these conformations. This high degree of structure variability makes ligand binding to a specific binding site more challenging since it is now possible for the protein to transiently block its own binding site. That is, there will be conformations where the region around the binding site is occupied by other segments of the protein, preventing a ligand from occupying that space. In order to explore if and how disordered proteins can provide complex signaling behavior to a network, we create a model of a simple disordered protein using principles from polymer physics.

TCR Diagram goes here!

## 2.3 Multisite Phosphorylation

Stuff about switch-like responses

Multisite phosphorylation specifically is a well-studied post-translational modification. This phenomenon occurs on both structured and unstructured proteins in many cell systems. CITE CITE CITE In signaling pathways, multisite phosphorylation often creates ultrasensitivity. cite, anything else? Ultrasensitivity creating a strong response from intermediate signals while reducing the influence of noise. CD3$\zeta$ - does give ultrasensitivity and we know it or it doesn't and we know it or we don't know? We want to explore if and how multisite phosporylation of disordered proteins conveys similar signaling functions.

## 2.4 Previous Modeling Attempts - FJC as Model for IDPs

Disordered proteins are commonly represented with models from polymer physics.examples of where this is actually true cite{VanValen2009} The distribution of end-to-end distances for disordered domains matches a worm-like chain (WLC) model with persistence length 3.04Å. This suggests $l_k = 0.6$nm....which is not what we use...not sure how to explain that one. [6] Models of disordered proteins freely-jointed chain (FJC) and WLC converge in the thermodynamic limit, with the persistence length for the WLC as half the Kuhn length used for the FJC. cite Something

Could explain why those models were developed - what are they good at describing

Alternative models for multisite phosphorylation of IDPs include molecular dynamic, ordinary differential equations, or particle based models. Cite times when each of these has been used However, FJC or other 'mesoscale' approaches reach timescales on the order of microseconds to seconds, which are computationally out of reach for traditional atomic scale MD. Cite time scales? This approach also allows us to capture the steric effects of a disordered chain, which are missed by coarser models. Do I need to cite stuff here?

Representations of disordered proteins as freely-jointed chains have already been used to elucidate properties of IDPs. The disordered molecule formin captures profilin-actin monomers and delivers them to the growing end of actin to aid in actin polymerization. In experimental studies of formin, pulling on the actin distal end of formin does not impact the actin polymerization rate. until large forces?, cite that paper An explanation of this phenomenon is explored in Bryant et al. 2016, where a force exerted on a freely-jointed chain extends the polymer, increasing capture of profilin-actin by increasing the availabiltiy of binding sites. This increase of capture rate balances the reduction in delivery rate to have a net zero impact on the actin polymerization rate.

### 2.5 The Big Question

# 3 Model Development

## 3.1 Freely Jointed Chain

We create a generic model of a disordered protein using a simplified $\theta$-solvent freely-jointed chain (FJC) from polymer physics. This model requires only specifying a number of rods (N) and a length per rod (Kuhn length, $\delta$ ). The FJC consists of N rigid rods of length $\delta$ which are allowed to perform a random walk where the only constraints are the chain length and connections. In our simulation, the FJC is allowed to explore its configuration space through randomized movements. The FJC model tracks where each joint is located, making steric interactions with the ligand easy to simulate compared to using the continuous WLC model. The ligand is simulated as an idealized sphere which may interact with the FJC. We compute quasi-equilibrium statistics of the chain and its bound or unbound ligands using a Monte Carlo (Metropolis) Algorithm.

where does this stuff go? Here? Assumptions?

In this model, the FJC is allowed to pass through itself. However, this turns out to be unimportant. Although the disordered protein would have a nonzero bond width, this size would be small in comparison to the kinase volume and volume of exploration space. If you consider two thin strings in 3-dimensional space, they will almost never intersect. Therefore, we model our polymer with infinitely thin width. Since it is infinitely thin, the time when it would take on a conformation where it overlaps itself is negligible compared to the number of legal conformations it assumes.

Additionally, we are only interested in the ensemble of configurations, not the dynamics. Therefore, the way the polymer achieves its conformations is unimportant to the results and any instances of self-intersection are negligible compared to the larger ensemble. Allowing the FJC to pass through itself, while unphysical, does not change the validity of our simulation.

### 3.2 Theoretical results

From detailed balance, which is what and we can use it why? the dissociation constants $K_D \equiv k_{\text{off}}/k_{\text{on}}$ of the floppy (native) state and the rigid (partially phosphorylated) state are

$$\frac{k_{on}}{k_{off}} = \exp\left(\frac{-\Delta G}{k_B T}\right) \tag{1}$$

$$\frac{K_{D_F}}{K_{D_R}} = \frac{K_F}{K_R} = \frac{\frac{1}{\exp\left(\frac{-\Delta G_F}{k_B T}\right)}}{\frac{1}{\exp\left(\frac{-\Delta G_R}{k_B T}\right)}} \tag{2}$$

$$\frac{K_F}{K_R} = \frac{\exp\left(\frac{-\Delta G_R}{k_B T}\right)}{\exp\left(\frac{-\Delta G_F}{k_B T}\right)} \tag{3}$$

$$= \exp\left(\frac{\Delta G_F - \Delta G_R}{k_B T}\right) \tag{4}$$

$$= \exp\left(\frac{(E_F - TS_F) - (E_R - TS_R)}{k_B T}\right) \tag{5}$$

$$= \exp\left(\frac{S_R - S_F}{k_B}\right) \tag{6}$$

$$= \text{ex}\left(\frac{(S^R_{on} - S^R_{off}) - (S^F_{on} - S^F_{off})}{k_B}\right) \tag{7}$$

$$= \exp\left(\frac{(k_B \ln(\frac{\Omega_R}{\Omega_R})) - (k_B \ln(\frac{\Omega_F P_F}{\Omega_F})}{k_B}\right) \tag{8}$$

$$= \frac{1}{P_F} \tag{9}$$

where $G_j = E_j - TS_j$ is the free energy of binding in the free or rigid state, $S_j = k_B \ln W$ is the entropy of binding, where W is the number of microstates and $P_j$ is the probability in the canonical ensemble that the configuration allows for binding. We let $\Omega$ be the total number of microstates, with $\Omega_F * P_F$ being the microstates available when the ligand is bound and $\Omega_R$ is the number of microstates available when the polymer is rigid. We also note $E_R = E_F$ since we are working at equilibrium. Since the perfectly rigid state always allows binding, $P_R = 1$, it is sufficient to compute $P_F$. We define $P_{occ}$ as the probability that the region of space needed by the kinase domain is occupied by some of the polymer. Thus, $P_{occ} = 1 - P_F$. Then

$$\frac{K_F}{K_R} = \frac{1}{(1 - P_{occ})}. \tag{10}$$

Our problem of interest is now reduced to computing the occlusion probability.

$$\frac{K_{D_F}}{K_{D_R}} = \exp\left(\frac{\Delta G_F - \Delta G_R}{k_B T}\right) \tag{11}$$

$$= \exp\left(\frac{S_R - S_F}{k_B}\right) \tag{12}$$

$$= \frac{1}{P_F} \tag{13}$$

## 3.3 Code Validation

There are theoretical solutions for many aspects of the freely-jointed chain. This provides a basis with which to verify our code.

### 3.3.1 Root-mean-square end-to-end distance

First, we look at the average end-to-end distance of the polymer (RMS). In our simulations, we normalize by the Kuhn length, so all simulations assume $\delta = 1$ and record all other parameters in units of Kuhn lengths. Therefore, we know from polymer physics that the RMS should increase as $\sqrt{N}$.

Average end-to-end distance (Root-mean-square end-to-end distance):

$$\sqrt{\langle r_{ee}^2 \rangle} = \sqrt{N\delta^2} = \delta\sqrt{N}$$

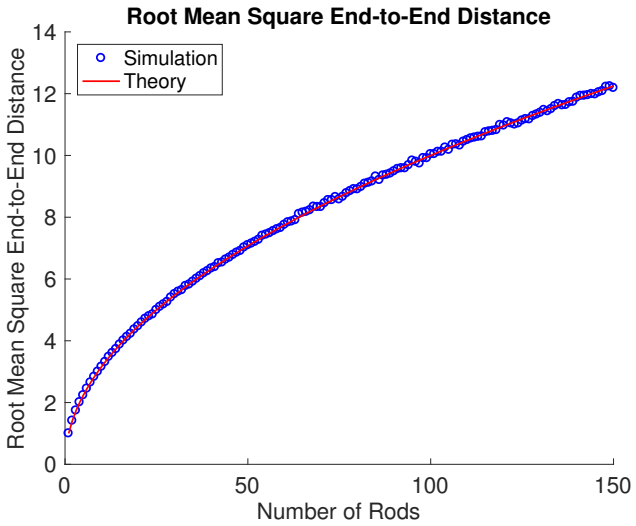


Figure 1: Theoretical root mean square end-to-end distance (red line) against simulated values (blue circles).

### 3.3.2 $R_{ee}$ Distribution

End-to-end distribution: [5]

$$P(r_{ee}) = 4\pi r^2 \left(\frac{3}{2\pi N\delta^2}\right)^{\frac{3}{2}} exp\left(\frac{-3r^2}{2N\delta^2}\right)$$

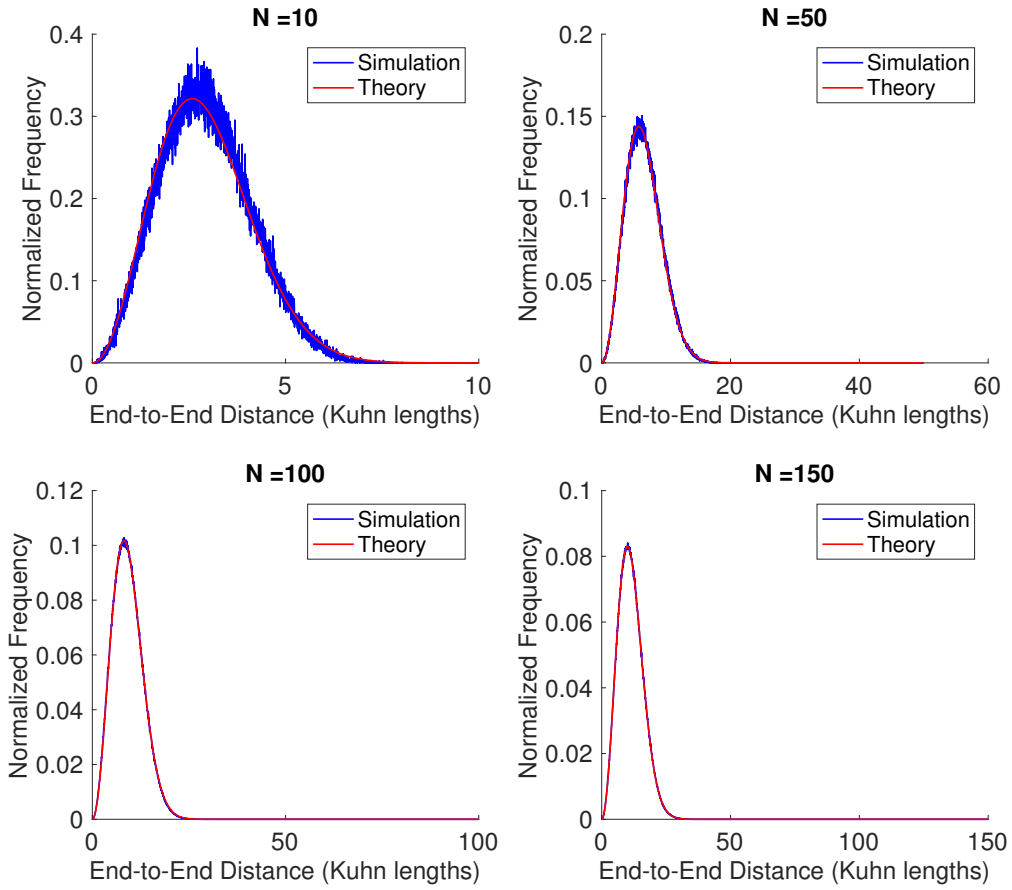


Figure 2: Simulated end-to-end distance distribution (blue) against theoretical distribution (red) for multiple polymer lengths (N).

cite something better than wikipedia?? and show derivation (?) of distribution formula?

#### 3.3.3 Occlusion Probability of End Site VS Analytical Result

### 3.4 Case Study: T Cell Receptor Zeta Chain

For the following study, we will focus on the mouse TCR CD3 $\zeta$ chain. The TCR CD3 $\zeta$ chain is a subunit of CD3 consisting of 164 amino acids. Of these, 21 are included in the signal peptide region of the protein. The remaining 143 amino acids make up the extracellular, transmembrane and cytoplasmic regions of the CD3 $\zeta$ chain. The cytoplasmic tail is an intrinsically disordered chain of 113 amino acids containing multiple phosphorylation sites, called ITAMs (immunoreceptor tyrosine-based activation motif). There are three ITAMs on the $\zeta$ chain, each containing two tyrosines. The tyrosine kinase Lck phosphorylates each tyrosine in the $\zeta$ chain and it is thought that phosphorylation of one site influences the binding of the kinase to other sites.

In mouse CD3 $\zeta$, the cytoplasmic tail spans residues 52-164 and the tyrosines are located at residues 72, 83, 111, 123, 142, 153. Therefore, if we were to renumber to begin at the beginning of the cytoplasmic tail, the region would be $N = 113$ amino acids long, with tyrosines located at $i = 21, 32, 60, 72, 91, 102$. (UniProt, entry P24161). Given an assumption of 0.3nm per Kuhn length (i.e. one Kuhn length is equivalent to one amino acid), then the tyrosines are similarly located along the 113 rods of the FJC.

Mouse Lck is composed of an SH3, SH2 and protein kinase domain, totaling 509 amino acids (61, 98, and 254 amino acids respectively, plus some small loops). (UniProt entry P06240). There is evidence that Lck is constitutively associated with CD4 and CD8 (membrane bound proteins) cite???. (Therefore, we only need to focus on the ability of the kinase domain to bind, since the other two Lck domains will be associated with CD4 or CD8. (Maybe???) Using a protein molecular mass calculator (http://www.bioinformatics.org/sms/prot_mw.html), we calculate that the kinase domain is 29.08 kDa. If we assume a protein density of 1.41 g / $cm^3$ cite???? then we can estimate the volume of the kinase domain:

$$(29 \times 1000\text{Da}) * (1.66 \times 10^{-27}\text{kg / Da}) * (1000\text{g / kg})/(1.41\text{g / cm}^3) = 34\,\text{nm}^3.$$

If we then approximate the kinase domain as a sphere, then we can estimate a radius:

$$\begin{aligned} V &= \frac{4}{3}\pi r^3 \\ 34\,\text{nm}^3 &= \frac{4}{3}\pi r^3 \\ r &\approx 2\,\text{nm} \end{aligned}$$

Measurements from the crystal structure of Lck suggest a volume of 45 $nm^3$ for the kinase domain. This estimate is on the same order of magnitude as our previous estimate. Note also, if we recalculate the kinase radius using a volume of $45\,\text{nm}^3$, we estimate a radius of 2.2 nm. Given an assumption of 0.3nm per Kuhn length, we represent Lck with a radius of seven Kuhn lengths.

# 4 Local structuring of disordered signaling proteins gives rise to cooperativity and sequential binding

## 4.1 Introduction

Intrinsically disordered proteins sterically occlude ligands by transiently sequestering the binding site.

There is evidence that indicates some IDPs undergo a disordered-to-ordered transition upon post-translational modification, i.e. phosphorylation. For example, phosphorylation of PAGE4 restricts the number of conformations it may explore, increasing rigidity of the backbone.[2] Post-translational modifications may also cause a conformational change, altering the availability of the binding site. The neural protein 4E-BP2 undergoes multisite phosphorylation which leads to a disorder-to-order transition, forming $\beta$ sheets which hide the eIF4E binding site. [1] Any other examples to include? tau protein!

We are interested in how cooperative effects may arise in reactions with a disordered protein. One model we explore is disorder-to-order transitions as a result of post-translational modifications. With regards to our case study, CD3$\zeta$, we assume that each phosphorylation event causes a fraction of the chain to undergo a disorder-to-order transition. We investigate how this local structuring phenomenon would impact subsequent phosphorylations by Lck along TCR CD3$\zeta$. Specifically, we want to know if local structuring of a disordered protein upon multi-site phosphorylation can induce enhancement of subsequent binding events.

## 4.2 Model and Methods

We model the TCR CD3ζ chain as a reely jointed chain, where each amino acid is represented as a segment. The unbound ligand is simulated as an idealized ghost sphere tangentially located at a single segment. Is it clear what this means? We calculate quasi-equilibrium statistics for the FJC and unbound ligand. For the CD3ζ chain, we simulate only the cytoplasmic region by an FJC with 113 segments. In our simulation, all lengths are normalized by the Kuhn length, so each rod has length 1 and the radius of the ligand is also measured in Kuhn lengths. We vary the size of the ligand. 3

We include local structuring as a limitation on which joints of the freely jointed chain are allowed to rotate. For each modified residue, some number of joints are effectively frozen in a straight conformation. The number of joints frozen per modification is a parameter we explore. This method of local structuring leaves the original binding site in a primarily available configuration, however, we are interested in how it impacts the neighboring modification targets (i.e. tyrosines to be phosphorylated)

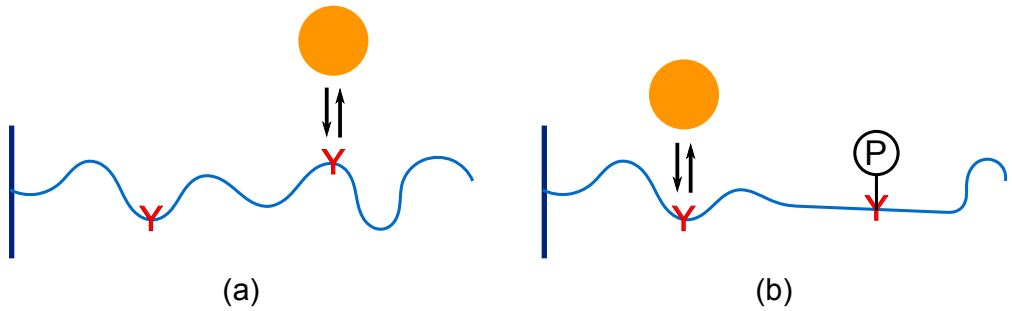


Figure 3: Cartoon of partial stiffening model. Entirely floppy FJC prior to modification (a) transitions to partially rigid chain after modification (b).

## 4.3 Results

### 4.3.1 Surface presence influences polymer configuration

Generally, FJCs are most likely to be in a 'hairball' conformation. From our simple model of a disordered protein, we may answer some basic questions. What is the probability that a ligand will be able to bind a specific site on a cytosolic disordered protein? How does this probability change when the protein is anchored to the membrane? How do these probabilities change with the contour length of the protein, size of the ligand, and where the binding site is located along the length of the protein?

We can see that in free space, the ligand is more occluded when there are more rods and/or the ligand is larger. These are both intuitive results. A longer chain creates more conformations where any location on the chain will be occluded by other segments. A shorter or less flexible chain will not be able to bend enough to bury a binding site. A larger ligand will require more space near the binding site to be open, which is naturally less likely. A binding site in the middle of the polymer will also be less available to ligand binding since it is more likely sheltered by the rest of the 'hairball' polymer. explain middle better

In half space, the polymer has fewer conformations it can take on since it can only occupy half of the region. This prevents many more 'hairball' conformations than it prevents straightened conformations. Overall, the effect is an overall straightening of the polymer in the presence of a membrane.

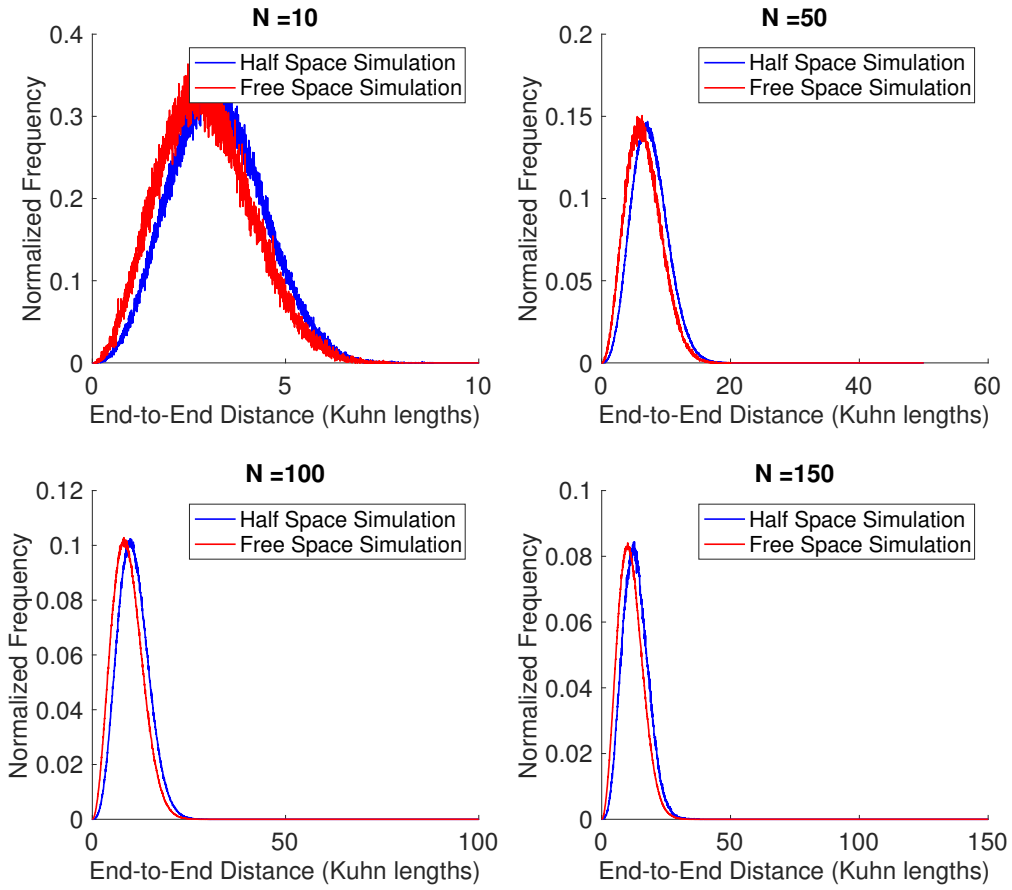


Figure 4: Distributions of polymer end-to-end distance in free space and half space for various polymer lengths (N). For each length, the end-to-end distance of the polymer in half-space is overall straighter than in free space.

### 4.3.2 Disorder inhibits ligand binding

The membrane increases the likelihood of straighter conformations, which would be likely to increase the binding probability. However, the membrane itself may also occlude the ligand since we include an orientation of the binding site in our simulation. Therefore if the binding site is oriented down towards the membrane, then even if the polymer is not occluding the ligand, the membrane still might. When we include a hard plane membrane in our simulation, we see that the presence of a membrane generally decreases the probability of ligand binding. When the ligand is small enough, the difference in binding probabilities between free space and half space binding is minimal.

Re-bin histograms Include image of simulation? Usually look bad....but might be a worthwhile visual. This is really ugly. Accidentally omitted last column? Color bars need to be fixed to be consistent somehow Color scales the same?

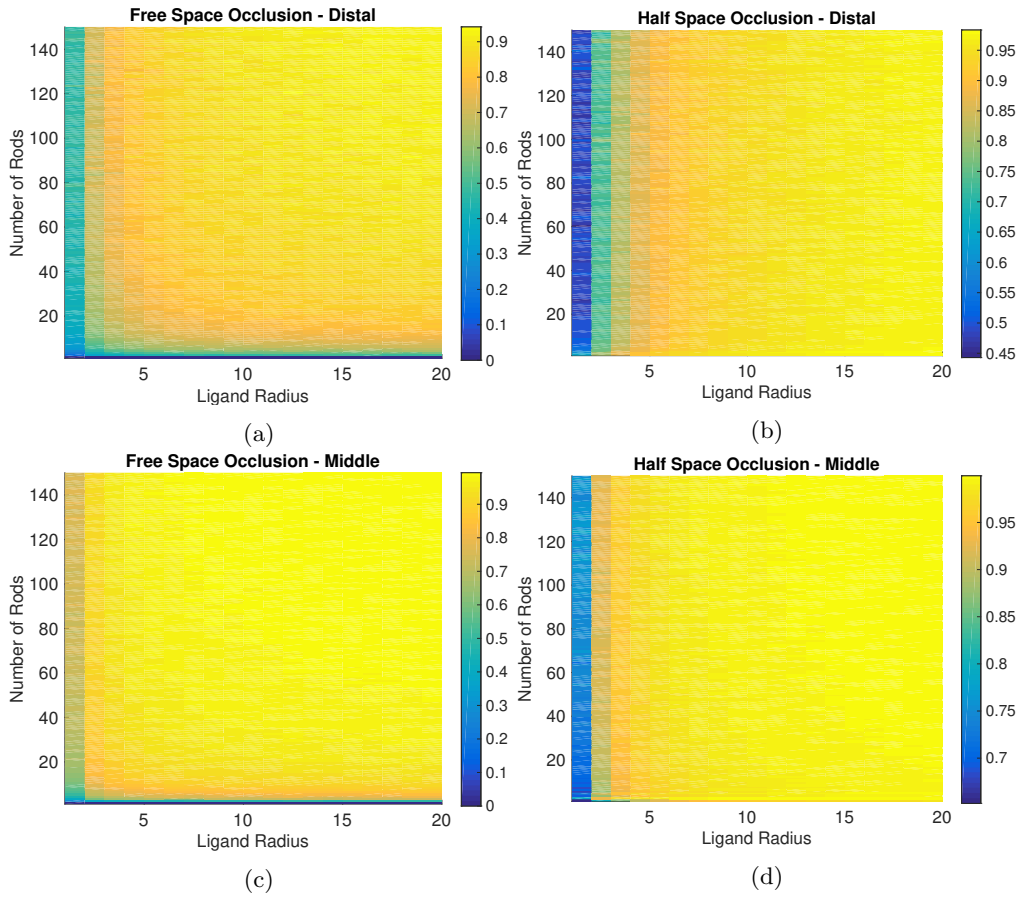


Figure 5: Probability of occluding a ligand of variable radius from a polymer of variable contour length when the binding site is at the distal end or middle of the chain in free space or half space. (a) Free space polymer with binding site at distal end. (b) Half space polymer with binding site at distal end. (c) Free space polymer with binding site in the middle. (d) Half space polymer with binding site in the middle.

#### 4.3.3 Cooperativity may arise from local structuring in intrinsically disordered proteins

If we assume that phosphorylation of tyrosines on the CD3$\zeta$ chain induces local structuring, then neighboring tyrosines will feel a reduction of entropic occlusion. This will cause them to be more available to binding by a ligand. The magnitude of this effect will vary based on how much structuring occurs, e.g. if it affects the nearest two residues or the nearest ten residues.

We see from these simulations that the average binding rate of a ligand to the unphosphorylated tyrosines increases as the number of phosphorylated tyrosines (and therefore the number of structured residues) increases. From the first to the sixth phosphorylation event, there is a 3-10 fold increase in the average binding rate for moderate (1/12 of chain length) to severe (1/6 of chain length) local stiffening per phosphorylation.

We have 10 fold change. Where does Omer's 100 fold change come in?

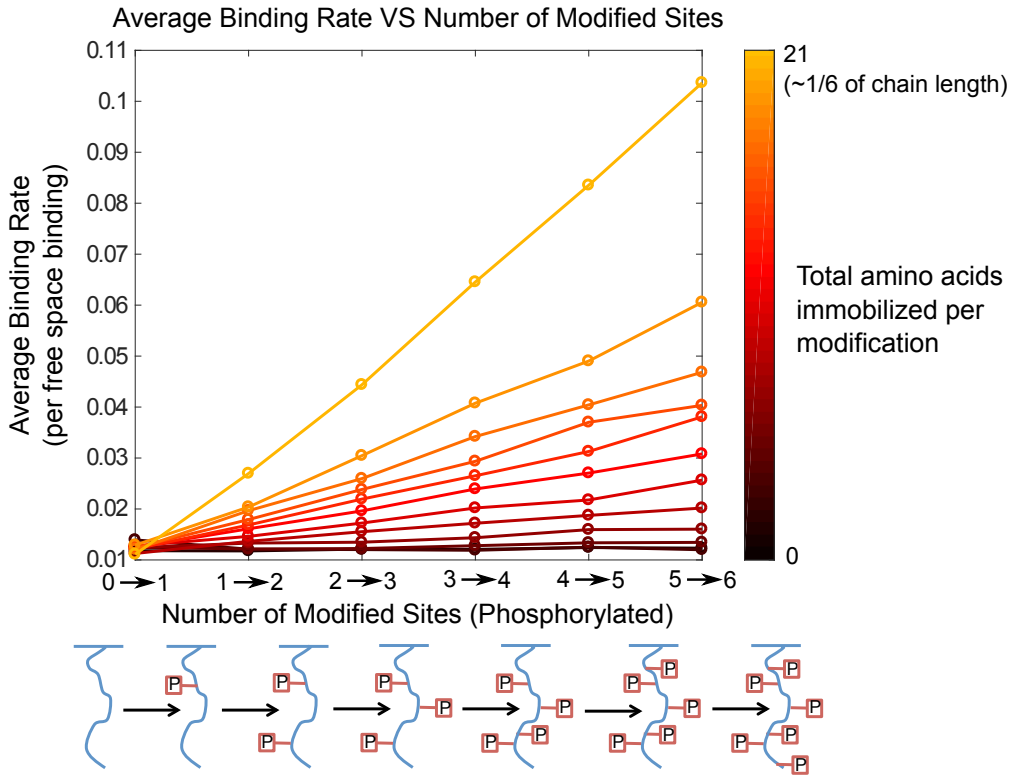


Figure 6: (Above) Simulated average binding rates of Lck to CD3$\zeta$ for different levels of phosphorylation given a specified degree of local structuring (none $\rightarrow$ black, low $\rightarrow$ red, high $\rightarrow$ orange). (Below) Cartoon representing a possible phosphorylation state series of CD3$\zeta$.

Local disordered-to-ordered transitions are sufficient to create positive cooperativity of PTMs. Positive cooperativity can increase the sensitivity of a response to changes in ligand concentration and increase the potency of signaling responses.

#### 4.3.4 Sequential binding naturally arises from polymer characteristics

We hypothesized that without any modifications due to binding, then with only the presence of a membrane, we would see preferential binding in an outwards to inwards (6-5-4-3-2-1) manner. In regards to our model system, that is to say we expected the tyrosine furthest from the membrane to be phosphorylated first and the tyrosine closest to the membrane to be phosphorylated last. We surmised this from the idea that tyrosine's too close to the membrane would see extra kinase inhibition from membrane occlusion, whereas the tail of the disordered protein would not experience this same effect.

When considering the partial stiffening model, we predict that this effect would be enhanced. In an unphosphorylated state, if the tyrosine furthest from the membrane is most likely to be bound, then partial stiffening would give increased preference to the next furthest from the membrane (here called the fifth tyrosine) as the second to be phosphorylated. This comes from the reduction of total configurations available to the protein. Since the stiffening would occur around the sixth tyrosine, the nearest unphosphorylated tyrosine would be the most affected. The segment of polymer near the fifth tyrosine would have fewer available conformations and therefore proportionately fewer would be occluding the fifth tyrosine.

Explain the above better. Not totally convinced that's the best argument. What's the correct term for 'unoccluded'? Available? Open?

Do we introduce this as a purposeful topic or as a neat thing that falls out? Include Dushek paper as benefit or as intro?

We obtained relative probabilities of binding for each tyrosine along the chain at each phosphorylation state. With this information, we are able to explore whether or not there is a dominant sequence of phosphorylation events. We ran a Gillespie algorithm with six events, one for each phosphorylation. From each run, we record which sequence or 'path' of phosphorylation. When we compile the path frequency data, it becomes clear that the first phosphorylation event is dominant. That is to say, any path beginning by phosphorylating the membrane distal tyrosine (6th tyrosine), will occur more often than any path beginning with the membrane proximal tyrosine.

For simplicity, we consider only the paths membrane proximal to membrane distal (123456) and distal to proximal (654321). We see that when a membrane is present, the probability of phosphorylating distal to proximal is much higher than that of phosphorylating proximal to distal. It is also more probable than if all paths were equally likely. This phenomenon is easily explained by the presence of a membrane. The membrane proximal tyrosine has a smaller range of space it may occupy than the distal tyrosine. Therefore, it is more likely to be close to the membrane in a configuration. Since the ligand cannot penetrate the membrane, tyrosines closer to the membrane have a higher probability of being effectively sheltered from ligand binding. This makes the distal to proximal path much more likely, regardless of local stiffening effects. This path preference is enhanced with local structuring since the distal tyrosine is more accessible and local structuring makes neighboring tyrosines even more available.

One would expect then, that a cytoplasmic disordered protein would not experience a path preference between N-terminal to C-terminal or vice versa. When we simulate CD3$\zeta$ without a membrane, there is still a marked preference for C-terminal to N-terminal phosphorylation. This effect arises from the spacing of the tyrosines along the polymer's length. As we noted above, the location of a tyrosine impacts how likely a ligand is to bind there. Since the tyrosines in CD3$\zeta$ are not equally spaced along the length of the protein, there is a bias for the tyrosine closest to one end, in this case the tyrosine closest to the C-terminal. When we simulate a polymer with the same length as CD3$\zeta$ but equally spaced tyrosines, we see that there is no longer a preference between the two paths.

We are soon going to introduce a ranking system for the paths in order to do a full analysis of all possible paths. This will help analyze the likelihood of any of the non-sequential paths.

Better to make one figure and label a,b,c in Inkscape?

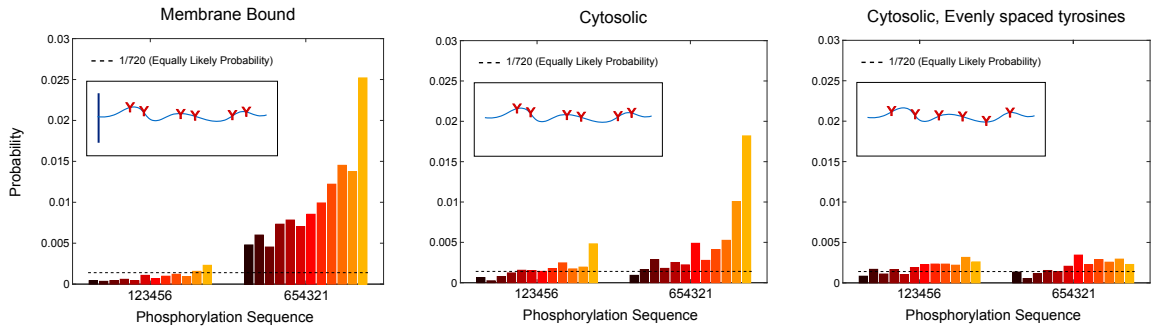


(a) (b) (c)

Figure 7: Probability of phosphorylating membrane proximal to distal (123456) compared with distal to proximal (654321). Equally likely probability of all paths indicated with black, dotted line. (a) CD3$\zeta$ parameters, with membrane. (b) CD3$\zeta$ parameters, without membrane. (c) CD3$\zeta$ length, evenly spaced tyrosine locations, without membrane.

Presence of a membrane inherently leads to sequential binding, a feature that plays a key role in creating or enhancing ultrasensitivity.cite

#### 4.3.5 Negative cooperativity may arise from local disordering of proteins

Paragraph about benefits? or is that for discussion? Paragraph about dephosphorylation

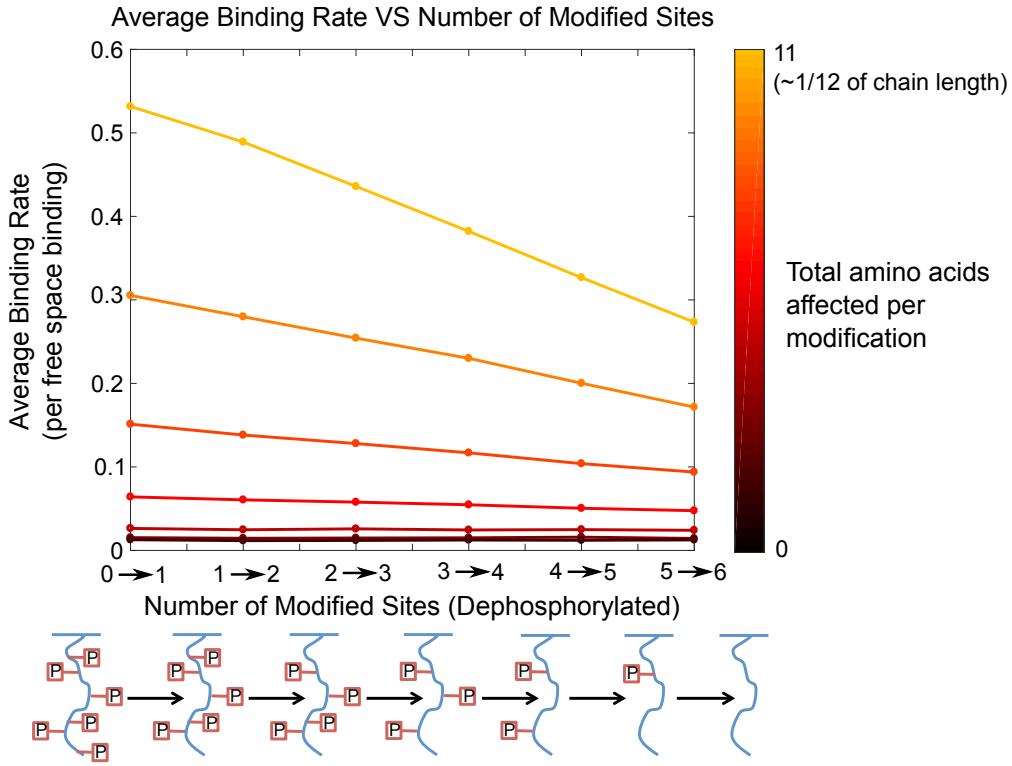


Figure 8: (Above) Simulated average binding rates of Lck to CD3$\zeta$ for different levels of dephosphorylation given a specified degree of local unstructuring (none $\rightarrow$ black, low $\rightarrow$ red, high $\rightarrow$ orange).

#### 4.3.6 Future Work: Quantifying cooperativity from reversible phoshphorylation with Hill coefficients

We will explore dephosphorylation/unstructuring of a fully rigid disordered protein.

We will create Hill curves of phosphorylation, dephosphorylation, and reversible phosphorylation. This will allow us to better understand and communicate our results with the rest of the biochemistry commmunity. In particular, the Hill curve of reversible phosphorylation will indicate if ultrasensitivity is achievable through this mechanism. true?

#### 4.3.7 Future Work: Exploring sequence of binding from dephosphorylation and reversible phosphorylation

### 4.4 Discussion

## 5 Electrostatics

### 5.1 Introduction

Subunits of many receptors have been shown to associate with the membrane prior to signalling. Others? Dobbins et al, Chenqi paper Close association with the membrane inhibits ligands from binding to their target site. Several of these chains have been shown to dissociate from the membrane after the extracellular receptor receives a stimulus. cite cite This mechanism may help prevent unwanted signaling. wording here is mediocre

In particular, evidence shows (CITE CITE CITE - Chenqi etc) that CD3$\zeta$ associates with the membrane prior to phosphorylation, sequestering the tyrosines in the bilayer. Post-phosphorylation, CD3$\zeta$ is no longer associated with the membrane, but remains anchored by its transmembrane region. Is this true without stimulus? what about stimulus without phosphorylation

Additionally, basic residue regions in the CD3$\zeta$ and $\epsilon$ chains play a major role in maintaining the association between the polymer and the membrane. Studies show that mutation of the basic residue regions is sufficient to cause the protein to dissociate from the membrane.cite Fully phosphorylated tyrosines are also sufficient to pull the protein away from the membrane, even when basic residue regions are present. cite

When the segment about mystery of where first signalling comes from

discuss clusters of TCR? future modeling question?

A molecular dynamics simulation of CD3$\epsilon$ indicates an approximately Gaussian distribution of the tyrosines, centered at the phospholipid heads of the membrane. [3]

evidence that fall off as feedback effect? Although the tyrosines will spend much of their time sequestered in the membrane, there is some probability of entropic forces ehhh transiently pulling them to the cytoplasm. hence distribution above.... When this occurs, Lck would be able to phosphorylate the tyrosine, creating a large negative charge on the chain. This phosphotyrosine would therefore repel the negative polar heads of the membrane, making it more favorable for that section of the polymer to pull out of the membrane.

We hypothesize that since there is some probability for this first event to occur, then after the first event there would be a cooperative enhancement of the probability of neighboring tyrosines becoming accessible. wording is terrible

hypothesis about sequential binding?

### 5.2 Model and Methods

We model the polymer-membrane association as a potential acting on each rod in a freely-jointed chain in half space. The potential only acts in the direction of the half space plane (in this case, z-direction). To develop the model, we need to explore parameter space to create potentials which display the same behaviors seen experimentally and through molecular dynamics. In particular, we want to match three conditions:

1. The polymer should display locational distributions consistent with Lopez et al. 2015. [3]

2. When basic residues are mutated, the polymer should dissociate from the membrane.

3. When all tyrosines are phosphorylated, the polymer should dissociate from the membrane.

Based on these goals, we group residues into four distinct categories: tyrosines, phosphotyrosines, basic residues, and remaining residues. Based on these groups, we develop a set of possible relationships to explore (Table).

Table 1: Notation for electrostatic potentials applied to different groups of residues.

| Residue Group | Electrostatic Potential Abbreviation |
|---|---|
| Tyrosines | $E_Y$ |
| Phosphotyrosines | $E_P$ |
| Basic Residues | $E_B$ |
| Remaining Residies | $E_R$ |

Table 2: Electrostatic potential relationships to explore for behavior matching experimental results.

| Group Number | Electrostatic Potential Relationship |
|---|---|
| 1 | $E_Y = E_B < 0$<br>$E_P = E_R = 0$ |
| 2 | $E_Y \neq E_B$<br>$E_Y < 0$<br>$E_B < 0$<br>$E_P = E_R = 0$ |
| 3 | $E_Y \neq E_B$<br>$E_Y < 0$<br>$E_B < 0$<br>$E_P > 0$<br>$E_R = 0$ |
| 4 | $E_Y = E_B < 0$<br>$E_P > 0$<br>$E_R = 0$ |
| 5 | $E_B < 0$<br>$E_Y = E_R = 0$<br>$E_P > 0$ |

Table 3: Cytoplasmic amino acid sequence of CD3$\zeta$ and $\epsilon$ chains. Basic residues (arginine, lysine, histidine) and tyrosines are highlighted separately in sequence. Relative numeric location in cytoplasmic sequence and fraction of residues from that group are noted.

| Chain | Group | Location in Cytoplasmic Sequence | Numeric Location | # / Total |
|---|---|---|---|---|
| CD3$\zeta$ | Basic Residues | RAKFSRSAETAANLQDPNQLYNELNLGRR EEYDVLEKKRARDPEMGGKQQRRRNPQE GVYNALQKDKMAEAYSEIGTKGERRR GKGHDGLYQGLSTATKDTYDALHMQTLAPR | 1,3,5,28,29,37,38, 39,41,48,51,52,53,60,65, 67,72,78,81,82,83,85,91, 99,102,106,113 | 29/113 |
| | Tyrosines | RAKFSRSAETAANLQDPNQLYNELNLGRR EEYDVLEKKRARDPEMGGKQQRRRNPQE GVYNALQKDKMAEAYSEIGTKGERRR GKGHDGLYQGLSTATKDTYDALHMQTLAPR | 21,32,60,72,91,102 | 6/113 |
| CD3$\epsilon$ | Basics Residues | WSKNRKAKAKPVTRGAGAGGRQRGQNKER PPPVPNPDYEPIRKGQRDLYSGLNQRRI | 3,5,6,8,10,14,21,23,27, 29,42,43,46,55,56 | 15/57 |
| | Tyrosines | WSKNRKAKAKPVTRGAGAGGRQRGQNKER PPPVPNPDYEPIRKGQRDLYSGLNQRRI | 38,49 | 2/57 |

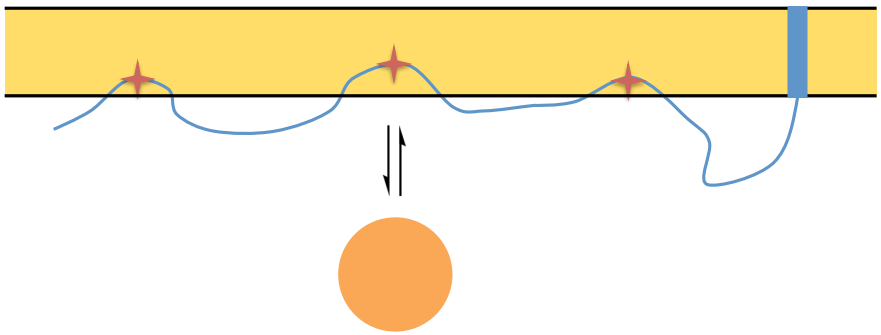

Figure 9: Cartoon of electrostatics model. COULD HAVE POTENTIAL IN CARTOON?. FJC associates with membrane, burying modification sites within membrane rendering them inaccessible to ligands.

### 5.2.1 Electrostatic Potentials

There are many more basic residues compared to tyrosines in both the CD3$\zeta$ and $\epsilon$ chains. Therefore, in order to account for tyrosine phosphorylation being sufficient to dissociate the polymer from the membrane, we would expect a repulsive force from the phosphorylated tyrosines. This directs our focus to Groups 3,4, and 5. Of these, we wish to look at the simplest cases first. Therefore we consider the case where tyrosines do not experience their own potential but experience the potential of either the basic residues or experience the same potential as the rest of the amino acids. Since tyrosines are not positively charged, it seems less likely that they would experience the same force as the basic residues. Although their aromatic ring structure may help to anchor the polymer to the membrane once associated with the membrane, it would not drive the polymer to the membrane to begin with. [3] Therefore we focus initial efforts on Group 5.

It's possible I didn't need any of the above about different groups.....'results not process' idea.

There are many types of electric potential we could explore for the correct behavior. Given that one of the phenomenons we wish to match is an approximately Gaussian distribution of both the tyrosines and polymer along the membrane edge, we use a parabolic-constant piecewise potential for our basic residues, instead of a Lennard-Jones potential.

Parabolic-constant piecewise potential:

Piecewise potential (aka, parabola-constant), ($PC$):

$$\begin{cases} width * z^2 - depth & z < \sqrt{\frac{depth}{width}} \\ 0 & z \geq \sqrt{\frac{depth}{width}} \end{cases}$$

We have two possible potentials for the remaining amino acids. In general, the peptide should not be able to penetrate deep into the membrane. Therefore, we can implement a hardwall or softwall constraint. The hardwall will prevent the remaining amino acids from passing the beginning of the membrane. A softwall constraint will allow amino acids to enter the membrane, but will incur an energetic penalty.

Hardwall:

$$\begin{cases} \infty & z < 0 \\ 0 & z \geq 0 \end{cases} \tag{14}$$

Softwall:

$$\begin{cases} k * z^2 & z < 0 \\ 0 & z \geq 0 \end{cases} \tag{15}$$

For the phosphorylated tyrosines, we will include an exponential distribution where the repulsive effect of the membrane drops off quickly as the phosphotyrosines move further away from the membrane.

Exponential decay:

go find actual equation to put here

$$\begin{cases} \infty & z \leq 0 \\ e^{-z} & z > 0 \end{cases} \tag{16}$$

## 5.3 Results

### 5.3.1 Model in which basic residues and tyrosines have similar energetics reveals puzzle in existing data

### 5.3.2 Initial parameter exploration of more general energetic model yields fit to polymer distribution

We initially want to match the distribution of the polymer to the molecular dynamics simulations from Lopez et al. We sweep through parameters for the basic residue potential and the softwall potential. The softwall potential permits a Gaussian curve for the tyrosine distributions. The hardwall condition (not shown) prevents the distributions from spreading below the zero axis where we have defined the membrane to be. When we explore these parameters, multiple possibilities for parameter sets emerge which meet the distribution conditions. Below are examples of distributions arising from our parameter exploration for both a tyrosine and a basic residue. We note that the potentials affect the distribution of the basic

residues more strongly than they affect the distributions of the tyrosines. From these parameter sets, we may refine our parameter search and begin exploring how the distributions are affected when all tyrosines are phosphorylated.

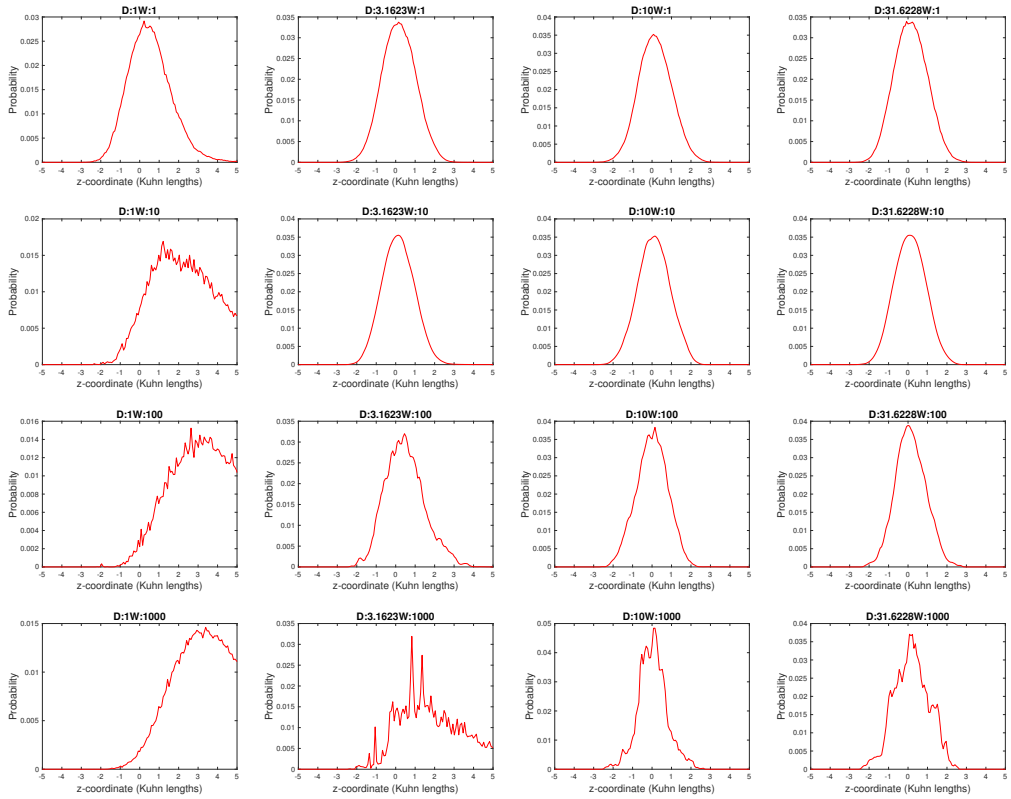


Figure 10: Tyrosine distribution resulting from parameter exploration of electric potentials. For this set, softwall potential is set at k=0.1. Basic residue potential depth ranges from $10^0$ to $10^{1.5}$.

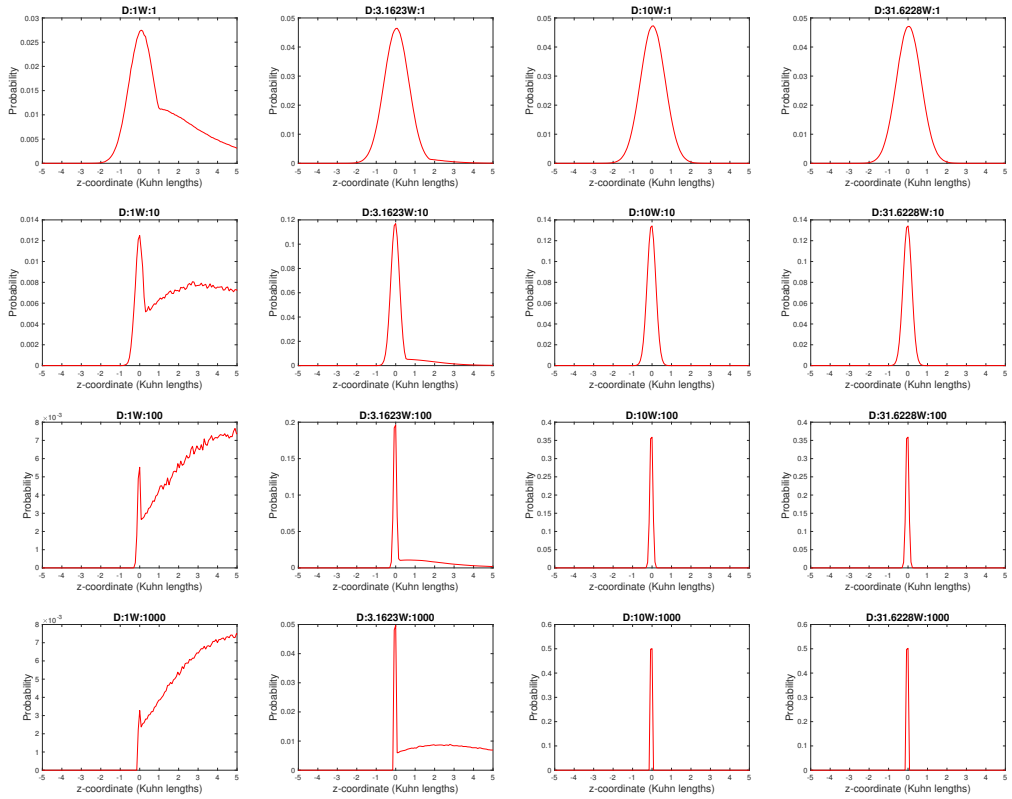


Figure 11: Basic residue distribution resulting from parameter exploration of electric potentials. For this set, softwall potential is set at k=0.1. Basic residue potential depth ranges from $10^0$ to $10^{1.5}$.

### 5.3.3 Future Work

First, we want to establish parameters (if they exist) which make our model exhibit the same behaviors as experimental and MD results. In particular, we now need parameters allowing the polymer to be free from the membrane when all tyrosines are phosphorylated. Either there will be only one reasonable parameter set which we can explore or there will be many parameter sets which display the desired properties. If there are multiple parameter sets then we may try to find other experimental results to narrow our parameter regime. Alternatively, we may explore two or three major parameter regimes: weakest, strongest, and median potentials. The results from a wide spread of parameters will give us an indication of how much the parameters matter to the qualitative results.

Second, with our parameter sets, we will now explore the effect of phosphorylation on the accessibility of successive tyrosines to a kinase. We wish to see if there is a cooperative enhancement of the binding rates based on phosphorylation of previous residues. Additionally, we will use this data to explore if there is a natural sequential binding sequence that arises. One would imagine that once a single tyrosine is phosphorylated then its nearest neighbor would be the most likely next target. However it is unclear if there is a first tyrosine that will be most likely to be phosphorylated and whether this will depend dominantly on basic residue distribution or on proximity to the transmembrane region.

paragraph about relating back to something useful or experimental?

### 5.4 Discussion?

# 6 Results: Simultaneous Binding

## 6.1 Introduction

Here we consider the case where ligands are able to bind to a polymer and remain bound. For instance, the SH2 domains of ZAP-70 bind to two tyrosines in an ITAM on CD3ζ and remain bound to phosphorylate downstream. cite!! This leads to the possibility that the polymer conformations are limited by the presence of a bound ligand, or even multiple bound ligands. We expect that as more ligands are added to the polymer, binding site occlusion will increase. The ligand may help to straighten out the polymer by limiting the number of conformations it can take on, but it will also occlude the binding site in many conformations. Depending on the size, number, and relative location of the ligand to the binding site, this effect may be stronger than the decreased occlusion via straightening.

## 6.2 Model and Methods

To simulate, each bound ligand is included as an idealized sphere tangentially bound to the polymer. The bound ligands rotate with the polymer and the polymer may not occupy the same space as the ligands. The bound and incoming ligands do not need to have the same radius. When a membrane is present, the bound ligand cannot penetrate the membrane.

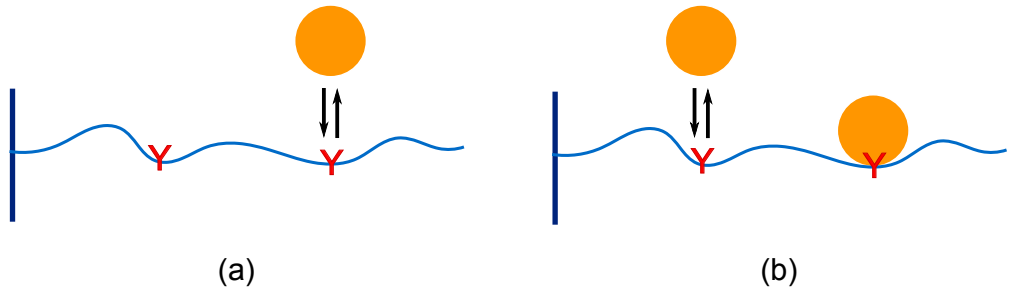


Figure 12: Cartoon of simultaneous binding model. FJC prior to ligand binding (a) transitions to FJC with single bound ligand and a second ligand attempting to bind (b).

## 6.3 Results

### 6.3.1 Negative cooperativity arises from simultaneous binding of ligands to an IDP

Find more examples of multiple binding

Once TCR CD3ζ is phosphorylated, the kinase ZAP-70 binds and phosphorylates the transmembrane protein LAT. CITE EVERYTHING! ZAP-70 is composed of two SH2 domains and a kinase domain.cite - - i.e. Wang et al 2010 or alternate These tandem SH2 domains each bind a phosphotyrosine on CD3ζ. Since minimally two SH2 domains must be able to bind to CD3ζ, it is natural to wonder how many domains could fit on a disordered chain and how each successive domain impacts the binding of another.

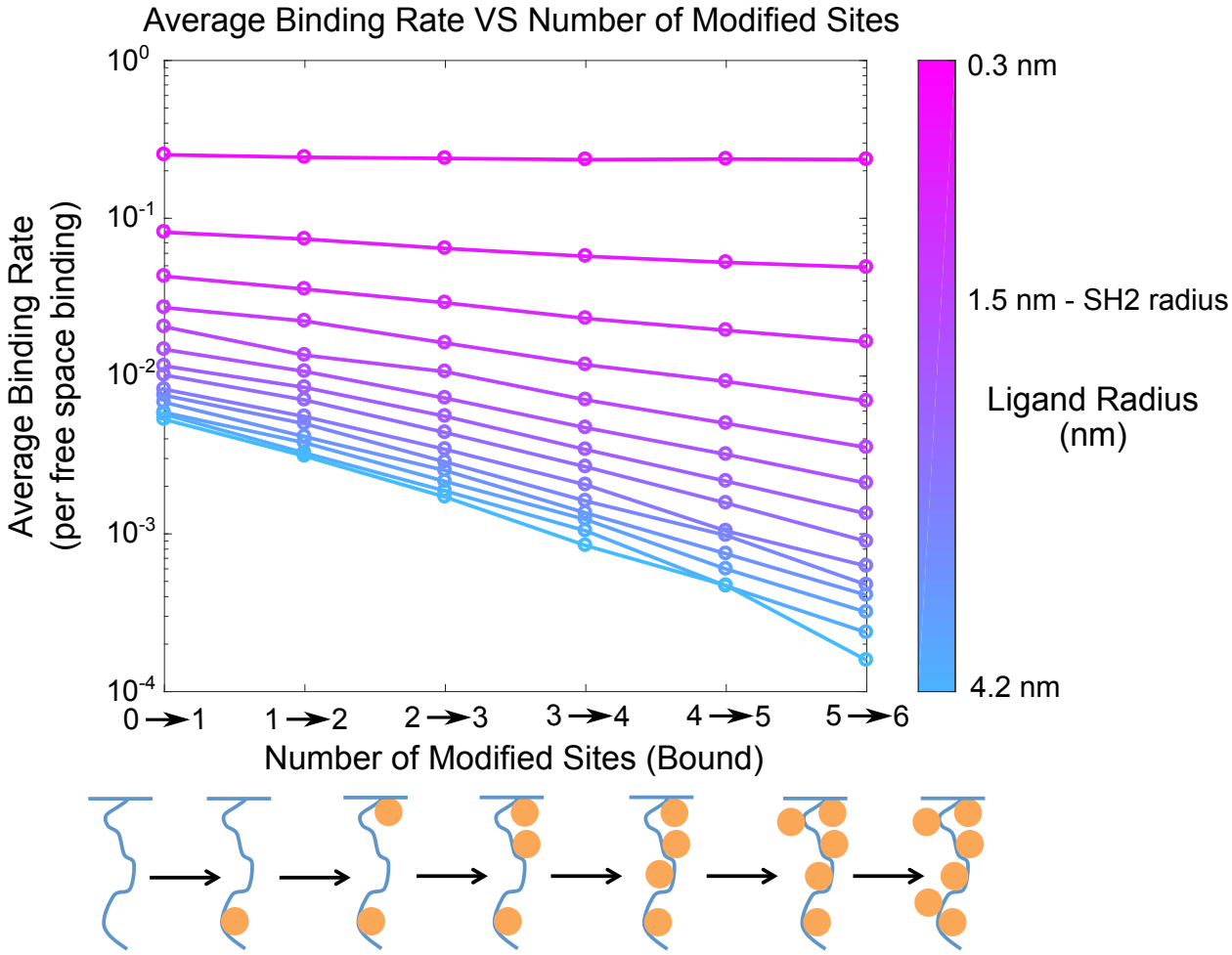


Figure 13: (Above) Simulated average binding rates of Lck to CD3$\zeta$ for specified number of SH2 domain sized (1.5nm radius) ligands previously bound and varying unbound ligand sizes (0.3 nm $\rightarrow$ pink, 4.2 nm $\rightarrow$ blue). (Below) Cartoon representing a possible bound configuration series of CD3$\zeta$.

There are two cases we may explore. The first assumes that each of the bound ligands is approximately the size of an SH2 domain and calculates the probability of a different ligand binding to one of the remaining binding sites. We investigate this for different sizes of ligand. Simultaneous binding of multiple SH2 sized domains will cause mild to severe negative cooperativity with the binding of another ligand. Larger ligands have a harder time binding when there are multiple SH2 domains already bound. For a 4.2nm radius ligand, there would be a 30 fold decrease in the probability of binding from having no other bound ligands to having five SH2 domains bound to the same disordered chain. Only very small ligands would be unhampered by the presence of other bound ligands.

An Lck molecule, only slightly larger than an SH2 domain, would experience an approximately eight fold decrease in its ability to bind once five SH2 domains are already bound to the disordered chain. This suggests the CD3$\zeta$ chain is mostly phosphorylated before ZAP-70 begins to attach or that phosphorylation by Lck slows down when ZAP-70 attaches. In the second case, this could lead to phosphorylation needing to occur via another mechanism, for instance via the kinase domain of ZAP-70 itself.

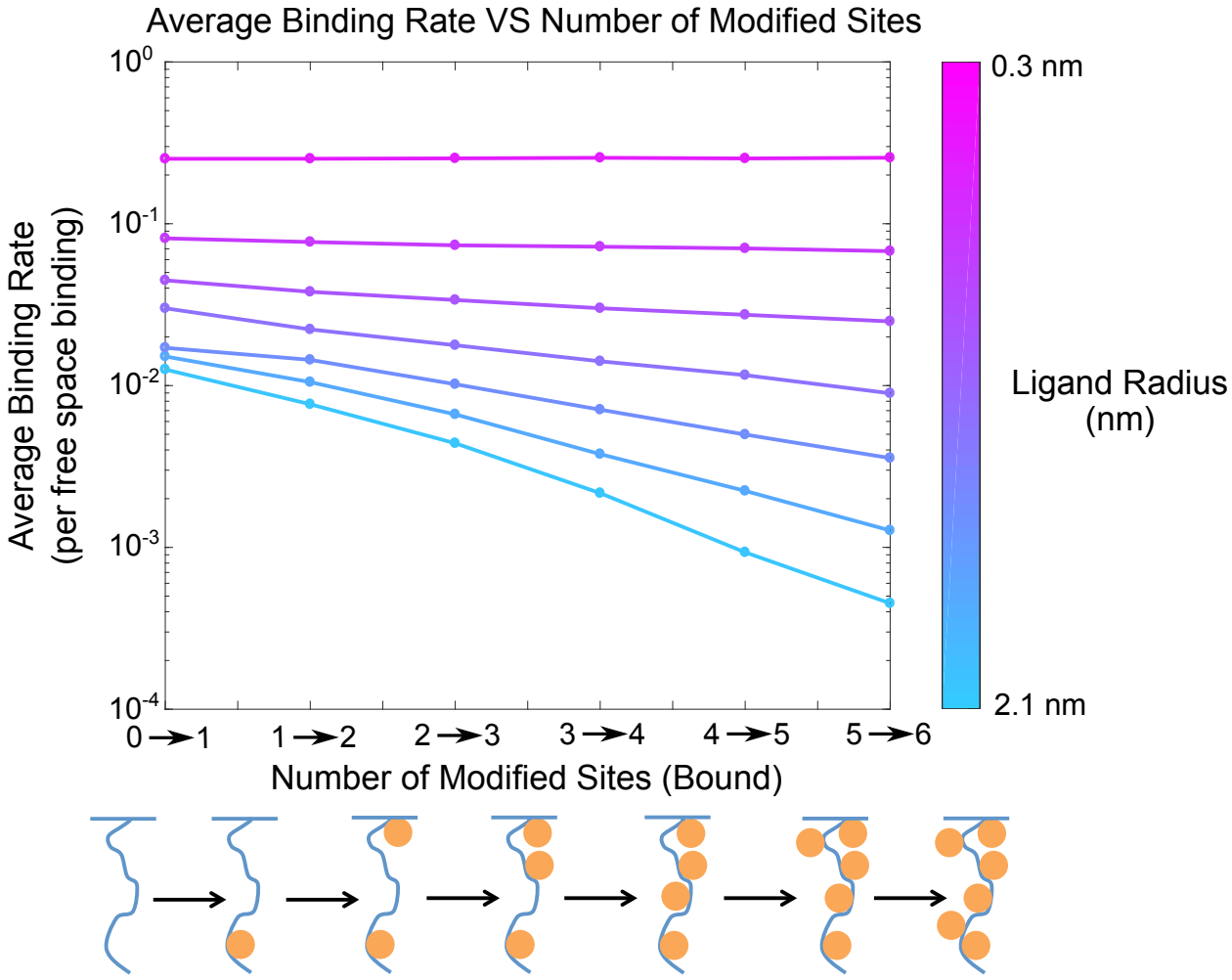


Figure 14: (Above) Simulated average binding rates of Lck to CD3$\zeta$ for specified number of ligands previously bound and varying ligand sizes (0.3 nm $\rightarrow$ pink, 4.2 nm $\rightarrow$ blue). (Below) Cartoon representing a possible bound configuration series of CD3$\zeta$.

The second case of simultaneous binding we explore is when only one ligand attaches to the disordered chain. We explore how having many bound ligands of a given size impacts another ligand of the same size binding. We see the same trend of behavior as above, but more dramatic. Here, if we investigate a ligand with radius 2.1nm, we already see a 30 fold decrease between no ligands bound and five bound. This is unsurprising since although a large bound ligand will straighten the polymer more, it will also create a much larger occluded volume making binding site accessibility much less likely. Note that similary, if the bound ligand size is less than that of an SH2 domain, then we actually see less negative cooperativity than above.

Simultaneous binding of ligands leads to negative cooperativity. This endows signaling systems with two features: high turnover of ligands even in high ligand concentration (which might be advantageous if ligands are involved in other reactions), and constant signaling activity in low ligand concentration. Similarly, this might reduce the impact of inhibitors, requiring much higher concentrations of inhibitor to completely turn off signaling.

Paragraph about benefits? or is that for discussion?

### 6.3.2 Future Work: Sequence of binding multiple ligands

rewrite this for simultaneous binding

We obtained relative probabilities of binding for each tyrosine along the chain at each bound state. With this information, we are able to explore whether or not there is a dominant sequence of binding events. We ran a Gillespie algorithm with six events, one for each ligand binding. From each run, we record which sequence or 'path' of binding. When we compile the path frequency data, it becomes clear that the first binding event is dominant. That is to say, any path beginning by binding to the membrane distal tyrosine (6th tyrosine), will occur more often than any path beginning with the membrane proximal tyrosine.

For simplicity, we consider only the paths membrane proximal to membrane distal (123456) and distal to proximal (654321). We see that when a membrane is present, the probability of binding distal to proximal is much higher than that of phosphorylating proximal to distal. This phenomenon is easily explained by the presence of a membrane. The membrane proximal tyrosine has a smaller range of space it may occupy than the distal tyrosine. Therefore, it is more likely to be close to the membrane in a configuration. Since the ligand cannot penetrate the membrane, tyrosines closer to the membrane have a higher probability of being effectively sheltered from ligand binding. This makes the distal to proximal path much more likely.

The preference for distal to proximal binding is enhanced by increasing ligand size. Larger ligands remain able to bind the membrane distal tyrosine with similar probability but will have a lower probability of binding tyrosines close to the membrane. When we simulate CD3$\zeta$ without a membrane, this preference is eliminated. Note that unlike with the local structuring model, a strict comparison of distal to proximal vs proximal to distal binding does not indicate a preference based on uneven spacing of tyrosines and in fact both of these paths are less likely than if all paths were equally probable. Although the most likely tyrosine to be bound is still the distal tyrosine, there is not a strong preference for the distal to proximal sequence because perfectly sequential binding is unlikely. Each bound ligand is more likely to sterically occlude a neighboring tyrosine than one further away. Therefore, if the distal tyrosine is the first bound, the next most likely to be bound is not its neighbor.

We are soon going to introduce a ranking system for the paths in order to do a full analysis of all possible paths. We look to answer if, for simultaneous binding, there a single path or group of paths that stand out as most likely.

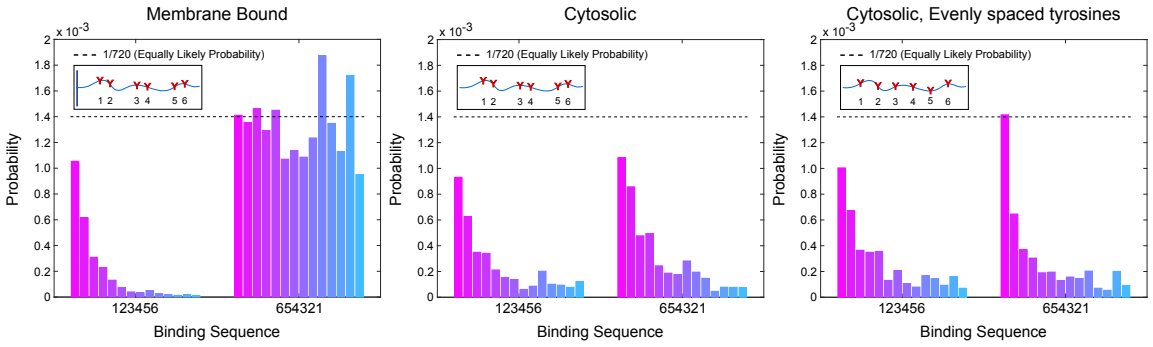


Figure 15: Probability of ligand binding membrane proximal to distal (123456) compared with distal to proximal (654321). Equally likely probability of all paths indicated with black, dotted line. (a) CD3$\zeta$ parameters, with membrane. (b) CD3$\zeta$ parameters, without membrane. (c) CD3$\zeta$ length, evenly spaced tyrosine locations, without membrane.

#### 6.3.3 Future Work: Multiple chains towards a full model of a T cell receptor signalosome

There is work showing that six ZAP-70 molecules bind to the disordered proteins of the T Cell Receptor on average. cite.... We want to eventually report an equilibrium value for the number of molecules able to bind to a CD3$\zeta$ chain. We will also expand our model to include all of the domains of the receptor. This will allow us to test if steric effects are sufficient to explain why only six ZAP-70 molecules would bind to the receptor simultaneously. When all of the chains are included in the simulation, each chain will be able to explicitly occlude a binding site on the opposite chain. With this, we will be able to answer questions of if or how disordered dimers impede binding.

### 6.4 Discussion

## 7 Role of the surface on tether-tether reactions within a signaling cluster

### 7.1 Introduction

#### 7.1.1 Tethering

Disordered proteins aid many reactions by acting as biological tethers. They may be permanent tethers tying two globular domains together or a domain to a surface example, example, cite cite. They may also be transient tethers, catching diffusing particles and tethering them to another molecule, i.e. formin. cite By tethering molecules or surfaces together, disordered domains effectively increase the local concentration of a particle. This increases reaction rates by improving the probability of two molecules bumping into each other through restriction of their diffusive domain.

Given that a surface reduces the exploration space of a molecule, it will naturally increase the local concentration without a tether. However, it will also reduce the accessibility of a molecule by sometimes occluding, for example, an enzymatic domain from reaching its substrate in the correct orientation. Given that the surface has both positive and negative effects on reaction rates, how does being tethered to a surface impact a reaction compared to being tethered to a smaller domain?

This type of interaction arises frequently with clustered reactions. For instance, the phosphorylation of a membrane tethered disordered domain by a membrane bound kinase. cite Experimental studies of such reactions are more easily performed on a sparse matrix such as dextran than on a hard surface. Therefore, it is important to understand the effect tethering to a surface has over tethering to a matrix. We explore how the presence of a surface influences the reach of a tethered domain and the overall local concentration.

#### 7.1.2 SHP-1

Paragraph about SHP1

reread SPR paper

## 7.2 Model and Methods

### 7.2.1 Model Tethers as Freely Jointed Chain

We explore the effects of a surface on three different tethers, each modeled as a freely-jointed chain characterized by their lengths as measured in Kuhn lengths. For each tether, we assume a Kuhn length,$\delta$, of 0.3nm, as supported by CITATION HERE. Given that these tethers are made up of PEG linkers and amino acids, each of which is approximately the size of a Kuhn length, the lengths of each tether may be approximated as $N$ Kuhn lengths, where $N$ is the total number of PEG linkers and amino acids. Note that we consider the size of biotin to be negligible for our simulation.

| Tether Name | Structure | N |
|---|---|---|
| PD-1 | (37392 B2) Bio-SRAARGTIGARRTGQPLKEDPSAVPVFSV DYGELDFQWREKTPEPPVPSVPEQTEY*ATIVFPSG | 64 |
| PEG-3 | Bio-(PEG)3-DLQEVTY*IQLDHH | 16 |
| PEG-28 | Bio-(PEG)28-DLQEVTY*IQLDHH | 41 |

### 7.2.2 SHP1 Parameters

We estimate the volume of SHP-1 based on its molecular weight, $67561 Da$, as listed in UniProt entry P29350. We use an average protein density of $1.41 g/cm^3$ (Fischer et al. 2004 Protein Sci).

$$(67.5 \times 1000\text{Da}) * (1.66 \times 10^{-27}\text{kg / Da}) * (1000\text{g / kg})/(1.41\text{g / cm}^3) = 79.468\,\text{nm}^3.$$

If we then approximate the phosphatase domain as a sphere, then we can estimate a radius:

$$\begin{aligned} V &= \frac{4}{3}\pi r^3 \\ 79.468\,\text{nm}^3 &= \frac{4}{3}\pi r^3 \\ r &\approx 2.7\,\text{nm} \end{aligned}$$

For comparison, we also estimate an upper bound on the radius of SHP-1 from PyMol measurements of the SHP-1 structure (PDB 3PS5). Rounding up for measurement error, the longest part of the structure is 86 Å. From this we calculate a maximum radius of $4.3 nm$.

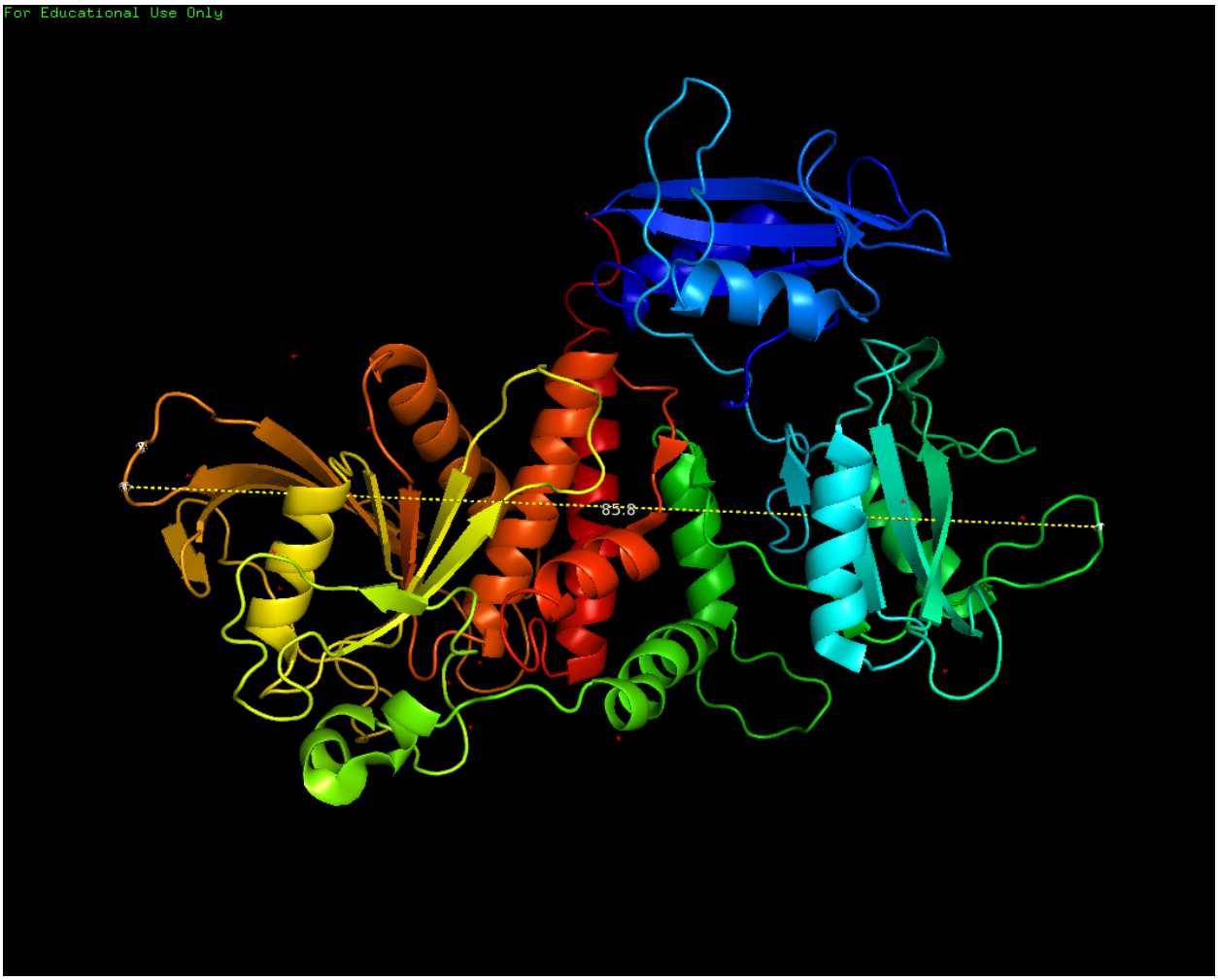


Figure 16: Measurement of maximum length (in Angstroms) of SHP-1 (PDB 3PS5).

Alternatively, we can estimate the volume of SHP-1 as a rectangular prism and then create a spherical approximation of equal volume. We estimate the length, width and depth of SHP-1 to be 76Å, 36Å, and 58Årespectively, giving a volume of 158688$Å^3$. From this, we calculate the radius for a spherical approximation to be 3.4nm.

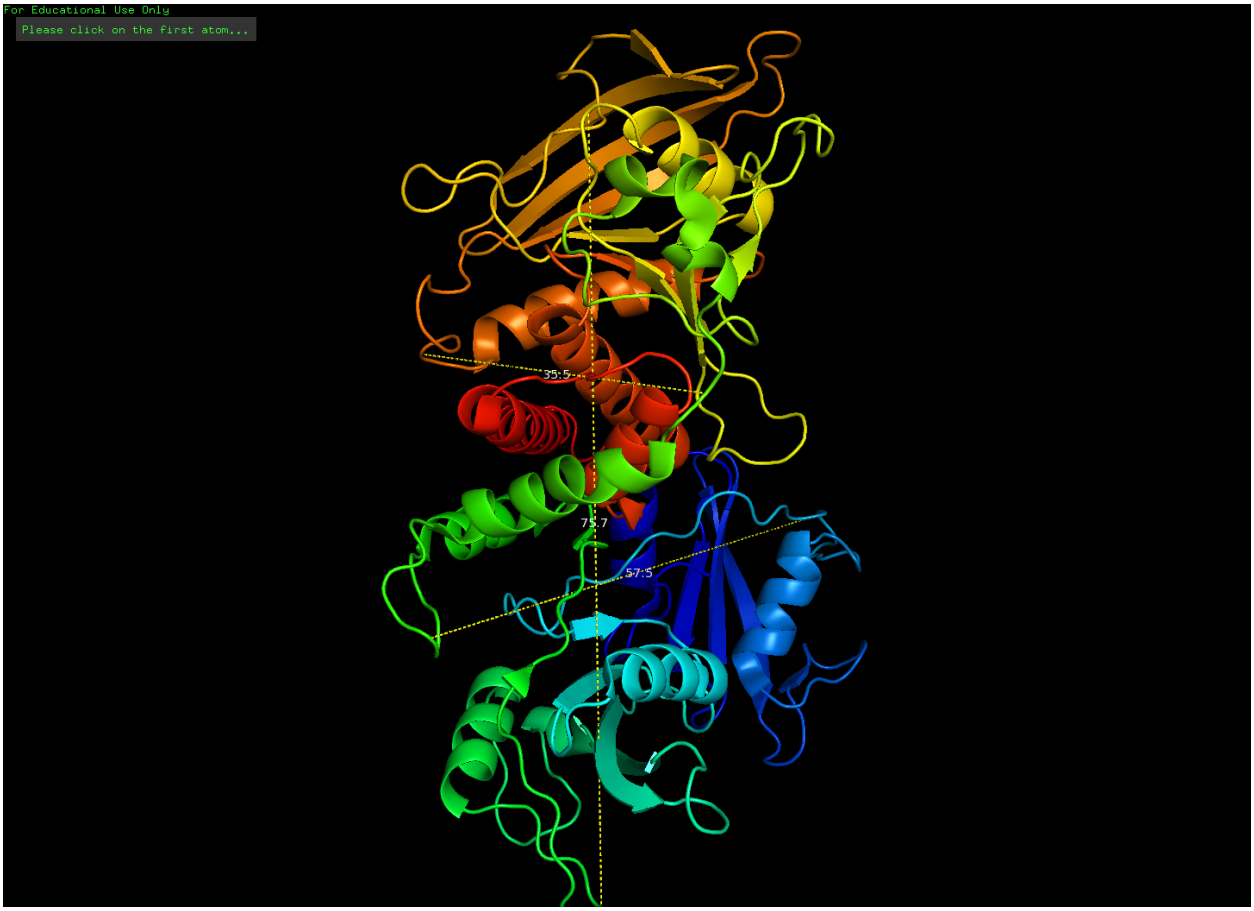


Figure 17: Measurement of rectangular dimensions (in Angstroms) of SHP-1 (PDB 3PS5).

Using the parameters estimated above, we simulate two equivalent tethers in free-space and half-space. The idealized SHP1 sphere, or ligand, is bound to the end of one of the tethers. The second tether has a ghost ligand attached in the same location. (Fig 3) We allow each tether to explore conformation space, at each conformation determining if the ghost ligand is occluded by the rest of the tether, or in half-space, by the half-space barrier. For the tether with the ghost ligand, we record both the location of the center of the ligand and whether or not it was occluded at each conformation. For the tether with the bound ligand, we only record the location.

The local concentration is alternately considered as the probability that the bound ligand is able to bind at the site of the ghost ligand within a small radius. I don't like this description To calculate this, we separate the the tethers from each other by a distance, $\rho$, measured in Kuhn lengths by adding $\rho$ to the $x$-coordinate of the ghost ligand. We then measure the distance between the two ligand centers, bound and ghost. If the centers are within a cutoff distance from each other AND the ghost sphere is not occluded, then the bound ligand is able to bind. This is calculated as a probability, which is then converted to a local concentration by dividing by the volume of the sphere defined by the cutoff radius.

Rewrite this section

The theoretical local concentration for two tethers a distance $\rho$ apart can be given by the following equation if both tethers are perfect worm-like chains:

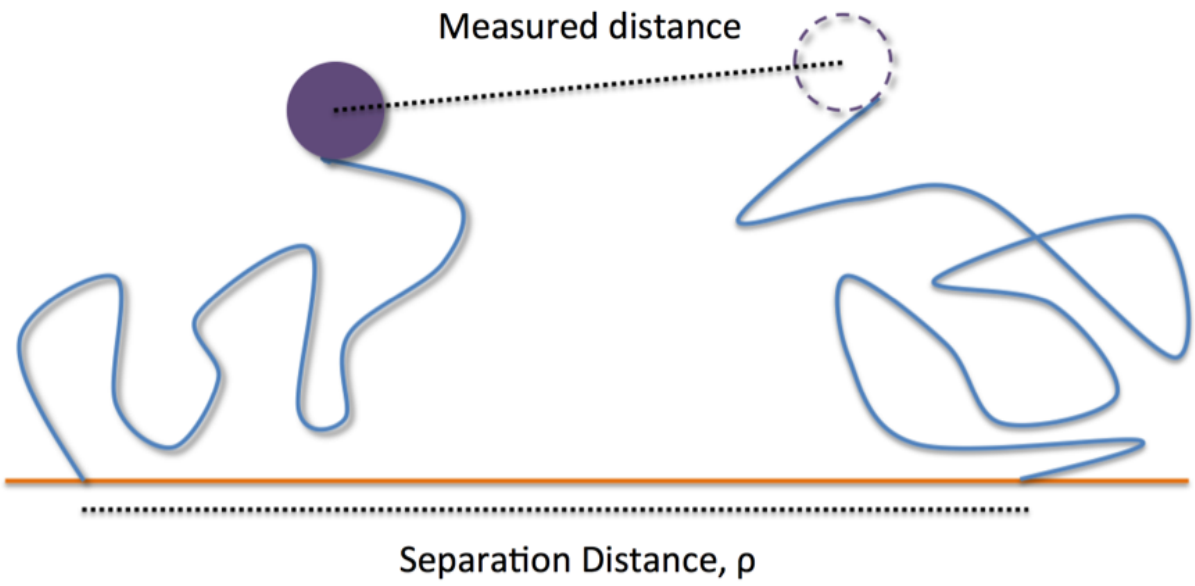


Figure 18: Cartoon of local concentration simulation in half space.

$$\sigma_{WLC}(\rho) = \left(\frac{3}{2\pi}\right)^{3/2} \frac{1}{L^3} e^{-\frac{3\rho^2}{2L^2}} \tag{17}$$

Experimentally, we measure the reaction rate $R(\rho)$. This equation is the product of a $k_{cat}$ and $\sigma(\rho)$. If the two tethers were perfect worm-like chains and the attached ligand did not impact the local concentration then when we fit the experimental $R(\rho)$ to $\sigma_{WLC}(\rho)$, we would have $R(\rho) = k_{cat}^{true} * \sigma_{WLC}(\rho)$. However, since this is unlikely to be the case, if we fit to the WLC theory curve anyway, then we actually have $R(\rho) = k_{cat}^{false} * \sigma_{WLC}(\rho)$. Instead, if we consider our simulated data to be the true local concentration and we fit a half-gaussian curve, $\sigma_{fit}(\rho)$, to the data, then we would have $R(\rho) = k_{cat}^{true} * \sigma_{fit}(\rho)$, where $\sigma_{fit}(\rho) = a * e^{-\rho^2/c^2}$.

We can use the simulated data to give an estimate of how incorrect $k_{cat}^{false}$ is compared to $k_{cat}^{true}$. We'll call this ratio $\kappa_{cat}$. Since we measured $R(\rho)$ experimentally, we must have:

This doesn't look super pretty

$$
\begin{aligned}
R(\rho) &= R(\rho) \\
k_{cat}^{false} * \sigma_{WLC}(\rho, L) &= k_{cat}^{true} * \sigma_{fit}(\rho, a, c) \\
\kappa_{cat} = \frac{k_{cat}^{false}}{k_{cat}^{true}} &= \frac{\sigma_{fit}(\rho, a, c)}{\sigma_{WLC}(\rho, L)} \\
\kappa_{cat} &= \frac{a * e^{-\rho^2/c^2}}{\left(\frac{3}{2\pi}\right)^{3/2} \frac{1}{L^3} e^{-\frac{3\rho^2}{2L^2}}} \\
\kappa_{cat} &= \frac{aL^3}{\left(\frac{3}{2\pi}\right)^{3/2}} \\
\kappa_{cat} &= \frac{a\left(\sqrt{\frac{3}{2}}c\right)^3}{\left(\frac{3}{2\pi}\right)^{3/2}} \\
\kappa_{cat} &= ac^3\pi^{3/2}
\end{aligned}
$$

if we assume? note? $c^2 = \sqrt{\frac{2}{3}}L^2 \implies L = \sqrt{\frac{3}{2}}c$.

| Model | Truth | Result |
|---|---|---|
| Worm-like chain | T | $R(\rho) = k_{cat}^{true} * \sigma_{WLC}(\rho)$ |
| Worm-like chain | F | $R(\rho) = k_{cat}^{false} * \sigma_{WLC}(\rho)$ |
| Half-gaussian fit | T | $R(\rho) = k_{cat}^{true} * \sigma_{fit}(\rho)$ |

We must therefore find appropriate $a$ and $c$ values for our half-gaussian fit in order to calculate the error.

### 7.2.3 Curve Fitting

Be consistent about $\sigma(r)$, $\rho$ etc.

To fit a half-gaussian curve to the simulation data, we use both Matlab's lsqcurvefit and fminsearch functions to fit the function $\sigma_{fit}(\rho) = a * e^{-\rho^2/c^2}$ to the data. The lsqcurvefit function uses the Trust-Region-Reflective Least Squares Algorithm by default whereas fminsearch uses the Nelder-Mead simplex algorithm. The Nelder-Mead algorithm provides parameters, aFit and cFit, that better fit the data compared to the Trust-Region-Reflective Least Squares Algorithm. When we run a parameter sweep to heuristically determine if these are the optimal parameters, we find that the sum of least squares obtain using $aFit$ and $cFit$ is consistently lower than that of the lowest found with any of our sweep parameters. Additionally, when we use the parameters which minimize the sum of least squares from our sweep to initialize the fminsearch function, our fit parameters change minimally and the sum of least squares differs by less than $10^{-10}$. For simplicity, we therefore use the fit parameters obtained from the Nelder-Mead algorithm.

Reference Lagarias et al. ?

clean up the language - too many fit parameters. Is it ok to reference them by function name vs algorithm name?

## 7.3 Results

### 7.3.1 Accessibility of a reaction site is reduced by the presence of a surface

Pick one of these? make one figure in inkscape to control spacing

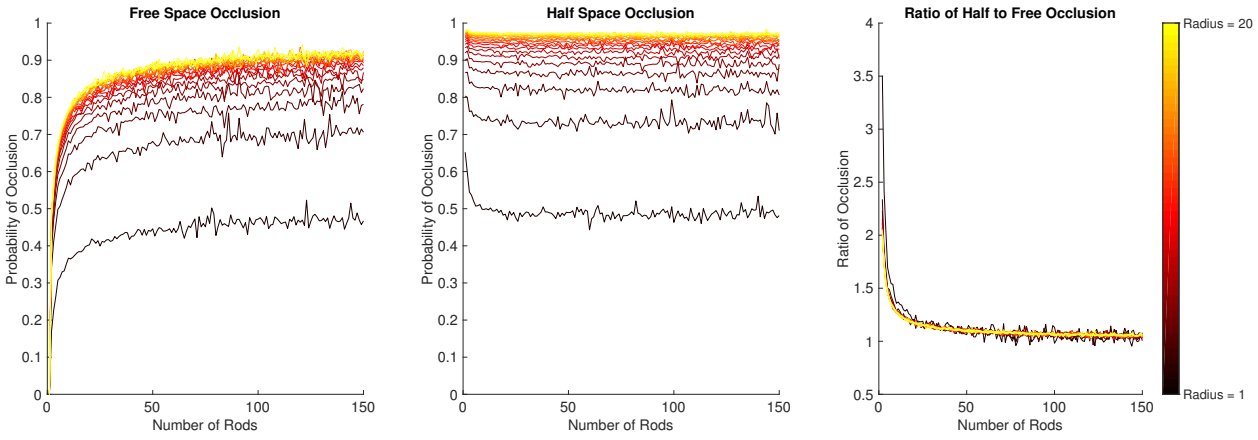


(a)

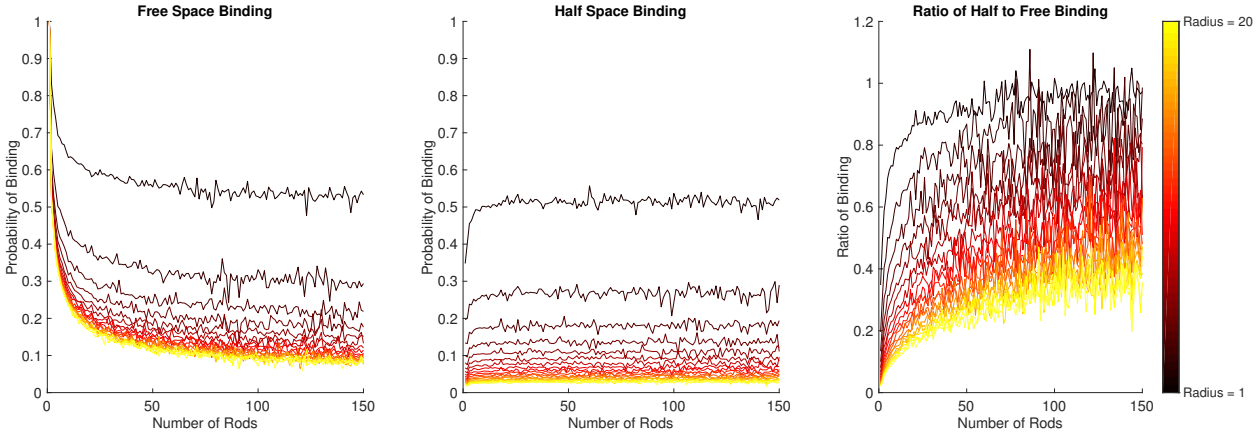


(b)

Figure 19

### 7.3.2 Reactions between tethered reactants are net enhanced by a surface

We explore how effective concentration is impacted by ligand size and polymer length, where effective concentration is a description of how often a ligand bound to the end of one polymer encounters a binding site on the end of a second polymer, with the two polymers separated by some distance. When ligand size is zero, or equivalent to no ligand attached to the polymer, then we see the free space polymers experience an effective concentration predicted by the worm-like chain model. Note that variability from the theoretical WLC curve is mitigated by decreasing the cutoff considered local. weird wording However, when we introduce a surface or ligand of nonzero size, the worm-like chain model no longer describes the effective concentration. We see that the surface enhances the effective concentration over the free space values but that a larger ligand size reduces the effective concentration.

Should really use SHP1 parameters for this figure.

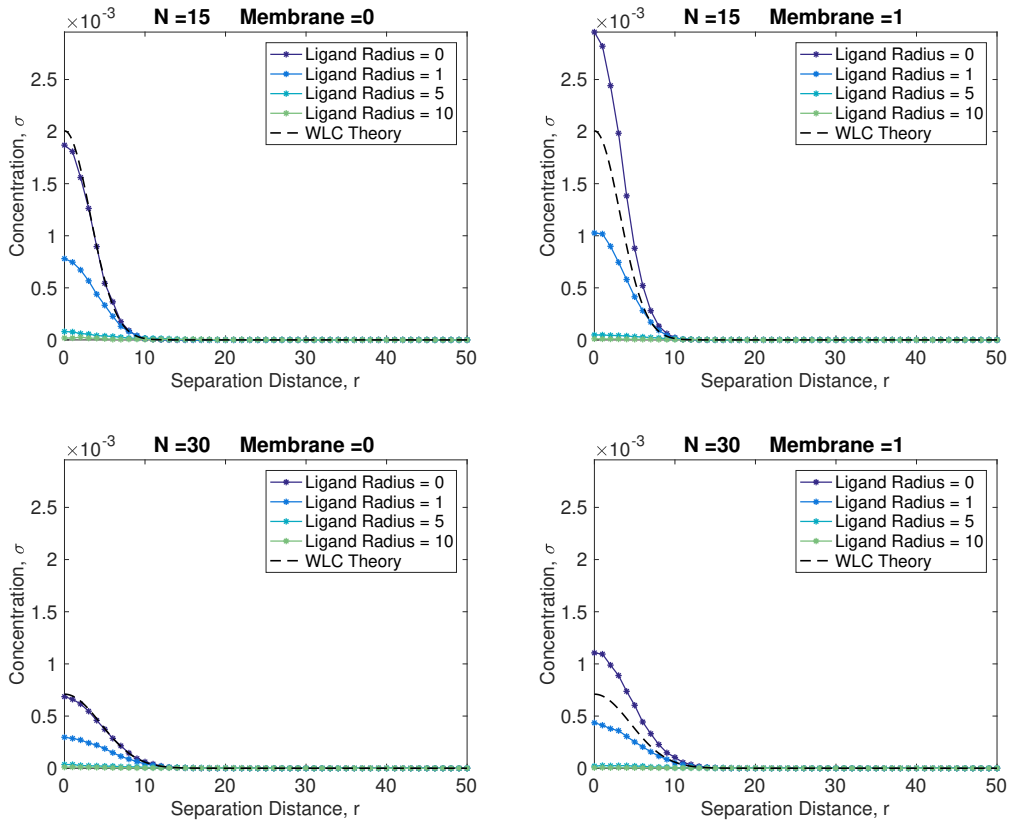
N =15 Membrane =0
N =15 Membrane =1
N =30 Membrane =0
N =30 Membrane =1
×10^-3
Concentration, σ
Separation Distance, r
Ligand Radius = 0
Ligand Radius = 1
Ligand Radius = 5
Ligand Radius = 10
WLC Theory

Figure 20

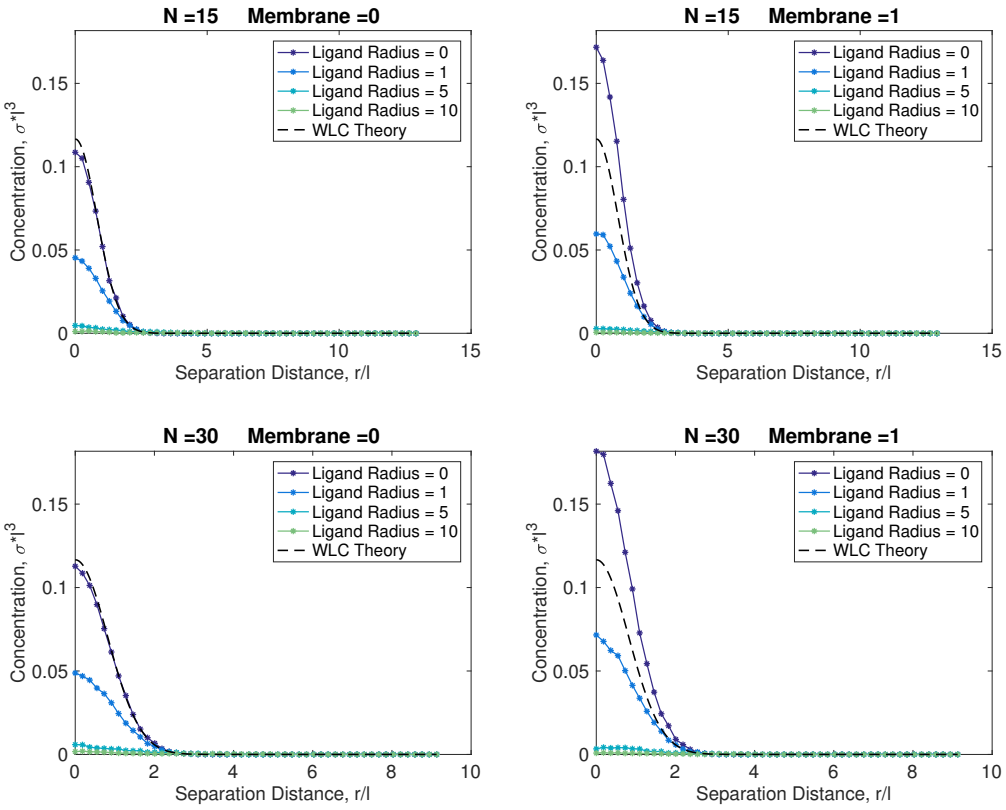


Figure 21

### 7.3.3 Reach parameter is unaffected by presence of surface

Our data shown earlier indicates that the presence of a surface will stretch a polymer compared to in free space. We would expect this straightening to also increase the reach parameter for the effective concentration. When we fit a half-gaussian curve to the simulated effective concentration curves, we find that the reach parameter, c, is unaffected by the presence of a surface. This parameter changes based on polymer length and ligand size, but is not impacted by a surface.

include curve fitting figure?

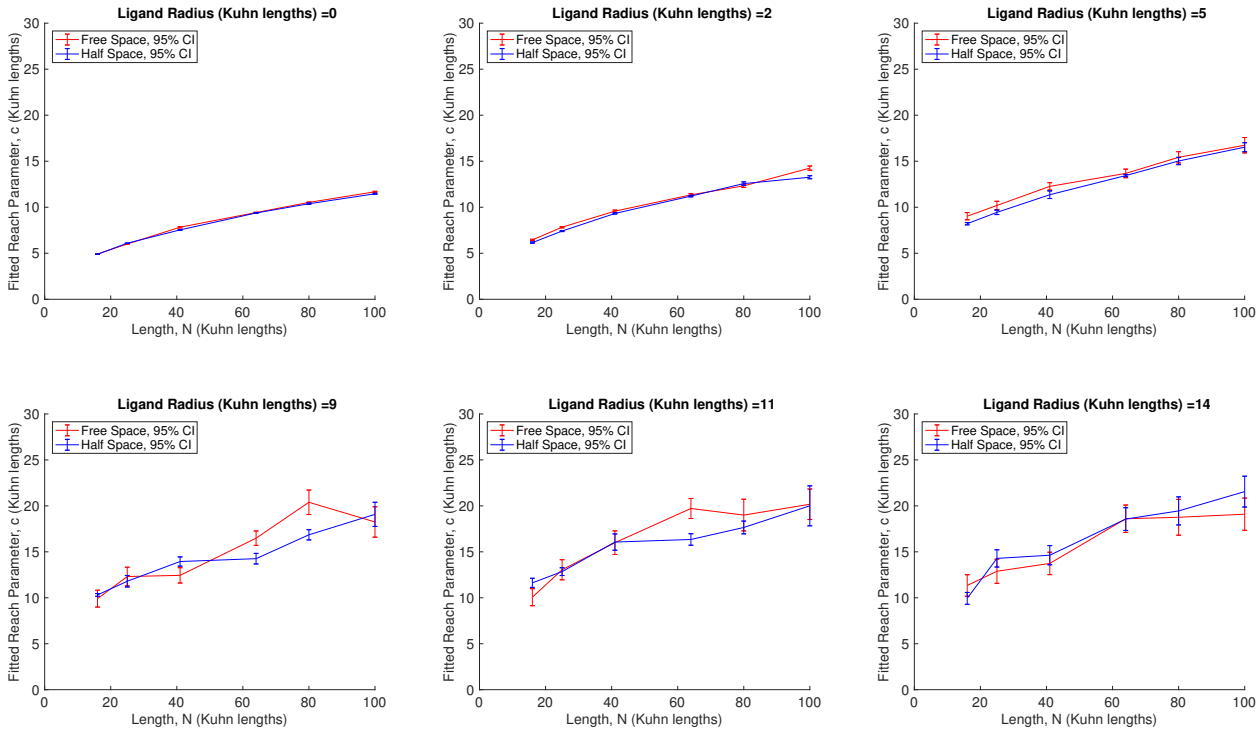
Reach Parameter in Free and Half Space
Ligand Radius (Kuhn lengths) =0
Ligand Radius (Kuhn lengths) =2
Ligand Radius (Kuhn lengths) =5
Ligand Radius (Kuhn lengths) =9
Ligand Radius (Kuhn lengths) =11
Ligand Radius (Kuhn lengths) =14
Free Space, 95% CI
Half Space, 95% CI
Fitted Reach Parameter, c (Kuhn lengths)
Length, N (Kuhn lengths)
0
5
10
15
20
25
30
0
20
40
60
80
100

Figure 22

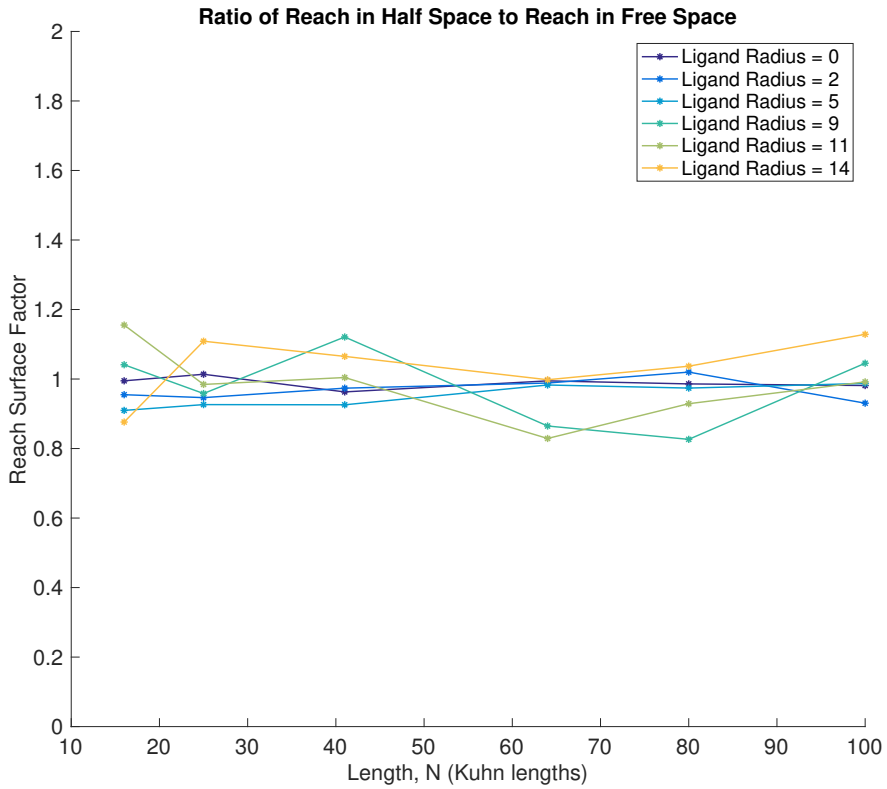


Figure 23

### 7.3.4 Matrix-bound versus surface-bound experiments confirm model predictions

### 7.3.5 Future Work: Catalysis surface factor $\kappa_{cat}^{(teth2teth)}$ versus $l_C$ and/or versus $r_{ligand}$

Experimental measurements of effective concentration do not distinguish between the effective concentration and the catalytic rate. Since these values are lumped into a single number, it is important to know how the surface impacts the apparent catalytic rate. This might be flat out incorrect. include calculation of how to find catalytic ratio? We will plot the ratio of apparent catalytic rates for various polymer lengths and ligand sizes. This will indicate if there is a relationship between the catalysis factor and the reaction parameters or if there is a single value describing the impact of the surface. The catalysis surface factor may then be used to determine how experiments on a surface differ from on a matrix and possibly give a conversion factor between the two.

### 7.4 Discussion?

# 8 Timeline

Table 4: Timeline of Coursework. Courses in italics do not count towards degree course requirements.

| **Fall 2014** | **Winter 2015** | **Spring2015** | **Summer 2015** |
|---|---|---|---|
| Dev Bio 212 | Dev Bio 212 | Dev Bio 212 | Research |
| Math 227A | Math 227B | Math 227C | |
| Dev Bio 203A | Dev Bio 232 | Dev Bio 203C | |
| Physics 230A | | M&MG 250 | |
| **Fall 2015** | **Winter 2016** | **Spring2016** | **Summer 2016** |
| *Math 205A* | *Math 205B* | *Math 205C* | Research |
| *Math 220A* | *Math 220B* | *Math 220C* | |
| *Math 230A* | *Math 230B* | *Math 230C* | |
| *Math 298A* | *Math 298B* | *Math 298C* | |
| **Fall 2016** | **Winter 2017** | **Spring2017** | **Summer 2017** |
| Dev Bio 212 | Dev Bio 212 | Dev Bio 212 | Research |
| Math 225A | Math 290B | CS 284C | Preliminary Exam |
| MMB 204 | | Physics 230B | Advancement |
| **Fall 2017** | **Winter 2018** | **Spring2018** | **Summer 2018** |
| Dev Bio 212 | Dev Bio 212 | Dev Bio 212 | Research |
| **Fall 2018** | **Winter 2019** | **Spring2019** | **Summer 2019** |
| Dev Bio 212 | Dev Bio 212 | Dev Bio 212 | Defense |

# 9 Appendix

## 9.1 Model Modifications

### 9.1.1 Stiffening

To include this model assumption, we modify the simulation in the following way:

1. Include binary sequence to indicate which sites are "stiff", sequence specified by user.
2. Create distance metric to indicate how far on either side of the site the effect extends, specified by user.
3. Include function to read binary sequence and create list of "stiff" joints, based on distance metric.
4. Prohibit joints on list from being chosen when simulation chooses joint to move.

### 9.1.2 Electrostatics

To include this model assumption, we modify the simulation in the following way:

1. Create binary sequence to indicate which sites are "phosphorylated".

2. Create distance metric to indicate how far on either side of the site the effect extends, specified by user.

3. Create function to read binary sequence and create list of which sites to ignore energy, based on distance metric.

4. Calculate energy of system based on Lennard-Jones or Piecewise potential curve plus hard or soft wall constraints.

   Polymer energy is the sum of the energy for each joint in polymer.

   Energy of sites on phosphorylated list are not included in the sum.

   Depth, width and wall/center location are specified by user.

5. Accept conformations that produce a lower energy than the previous conformation.

6. Reject with normal probability any conformations with higher energy than previous conformation.

7. Rejection keeps polymer in previous conformation, but goes on to next time step. (Metropolis step.)

### 9.1.3 LJ Parameter Optimization

First potential:

Lennard-Jones potential, ($V_{LJ}$):

$$V_{LJ} = 4\epsilon \left( \left( \frac{l_D}{r - r_W} \right)^{12} - \left( \frac{l_D}{r - r_W} \right)^{6} \right)$$

where $\epsilon$ is the well depth, $l_D$ is the Debye length, $r_W$ is the potential wall location (vertical asymptote), and $r$ is the location of the joint in question. For our purposes, $r$ is the z-coordinate of the joint in question.

We want to look at what Debye length causes the electrostatic potential minima to shift from before $r = 0$ to after $r = 0$ (before, after membrane). We therefore solve the derivative of $V_{LJ}$ (given below) for $l_D$ when $r = 0$ and $dV_{LJ}/dr = 0$.

The derivative of $V_{LJ}$:

$$\frac{dV_{LJ}}{dr} = 4\epsilon \left( l_D^{12} \frac{-12}{(r - r_W)^{13}} + l_D^{6} \frac{6}{(r - r_W)^{7}} \right)$$

Input $dV_{LJ}/dr = 0$, $r = 0$:

$$
\begin{aligned}
0 &= 4\epsilon \left( l_D^{12} \frac{-12}{(-r_W)^{13}} + l_D^6 \frac{6}{(-r_W)^7} \right) \\
0 &= \left( l_D^{12} \frac{-12}{(-r_W)^{13}} + l_D^6 \frac{6}{(-r_W)^7} \right) \\
l_D^{12} \frac{12}{(-r_W)^{13}} &= l_D^6 \frac{6}{(-r_W)^7} \\
l_D^6 \frac{12}{(-r_W)^{13}} &= \frac{6}{(-r_W)^7} \\
12 * l_D^6 &= 6 * (-r_W)^6 \\
l_D^6 &= \frac{(-r_W)^6}{2} \\
l_D &= \sqrt[6]{\frac{1}{2}} * |r_W|
\end{aligned}
$$

Note that if the potential wall location is negative, then the Debye length may be either positive or negative. If the wall location is positive, then for our simulation, there is no Debye length that would cause the potential minimum to fall at $r = 0$.

Therefore, we can say that when $l_D < \sqrt[6]{\frac{1}{2}} * |r_W|$ then the polymer will be preferentially located 'under the membrane', or with $r < 0$ for most of its rod locations. Similarly, for $l_D > \sqrt[6]{\frac{1}{2}} * |r_W|$, the polymer will primarily be 'above' the membrane.

#### 9.1.4 Simultaneous Binding

To include this model assumption, we modify the simulation in the following way:

1. Create "bound ligands", with location and radius specified by user. (Location specified by file or binary sequence.)
2. Bound ligands occlude polymer, rejecting conformations that intersect the ligand sphere.
3. Bound ligands occlude each other, rejecting conformations where two ligands intersect each other.
4. If there is a membrane, bound ligands may not fall below membrane, rejecting conformations where this occurs.
5. Rejecting conformations does not step time forward. Continue looking for conformations until one meets constraints.
6. Binding sites are considered 'occluded' if a bound ligand intersects the binding site sphere.
7. Binding sites located where bound ligand is located read as always occluded.

### 9.2 Assumptions

### 9.3 Gillespie Algorithm

## References


[1] Alaji Bah et al. "Folding of an intrinsically disordered protein by phosphorylation as a regulatory switch." In: *Nature* 519.7541 (2015), pp. 106–9. ISSN: 1476-4687. DOI: 10.1038/nature13999. URL: http://dx.doi.org/10.1038/nature13999%7B%5C%%7D5Cnhttp://www.pubmedcentral.nih.gov/articlerender.fcgi?artid=2842604%7B%5C&%7Dtool=pmcentrez%7B%5C&%7Drendertype=abstract%7B%5C%%7D5Cnhttp://www.nature.com/doifinder/10.1038/nature13999%7B%5C%%7D5Cnhttp://www.ncbi.nlm.nih.gov/pubmed/20298971%7B%5C%%7D5Cnhttp://w.

[2] Yanan He et al. "Phosphorylation-induced conformational ensemble switching in an intrinsically disordered cancer/testis antigen". In: *Journal of Biological Chemistry* 290.41 (2015), pp. 25090–25102. ISSN: 1083351X. DOI: 10.1074/jbc.M115.658583.

[3] Cesar A Lopez et al. "Membrane-Mediated Regulation of the Intrinsically Disordered CD3$\epsilon$ Cytoplasmic Tail of the TCR". In: *Biophysical Journal* 108.May (2015), pp. 2481–2491. ISSN: 00063495. DOI: 10.1016/j.bpj.2015.03.059.

[4] P Tompa and K-H Han. "Intrinsically disordered proteins". In: *Physics Today* 65 (2012), pp. 64–65. ISSN: 0968-0004. DOI: 10.1016/j.tibs.2012.08.004.

[5] David Van Valen, Mikko Haataja, and Rob Phillips. "Biochemistry on a leash: The roles of tether length and geometry in signal integration proteins". In: *Biophysical Journal* 96.4 (2009), pp. 1275–1292. ISSN: 00063495. DOI: 10.1016/j.bpj.2008.10.052. URL: http://dx.doi.org/10.1016/j.bpj.2008.10.052.

[6] Huan Xiang Zhou. "Loops in proteins can be modeled as worm-like chains". In: *Journal of Physical Chemistry B* 105.29 (2001), pp. 6763–6766. ISSN: 10895647. DOI: 10.1021/jp011355n.